

Development and Characterization of Silymarin Phospholipid Complex for Improved Solubility, and Toxicological Evaluation in Experimental Animals

Mandeep Kumar Singh, Umesh Kumar Patil*

Department of Pharmaceutical Sciences, Dr. Harisingh Gour Vishwavidyalaya (A Central University), Sagar, Madhya Pradesh, INDIA.

ABSTRACT

Objectives: The silymarin phytosome (SPY) was developed to improve the solubility and dissolution. The prepared phytosome was evaluated for hemolytic, membrane stabilization activity, and *in vivo* acute and sub-chronic toxicity. **Materials and Methods:** The toxicological evaluation was carried out by assessing its effects on liver, kidney, brain, lungs, heart and spleen in a rat model. In addition to confirmation of formation of phytosome, the physical-chemical characterization was done by FTIR, DSC, PXRD, and ¹H NMR. **Results:** The optimized formulation has higher aqueous solubility of SPY compared to that of pure silymarin. The formulation also exhibited a significantly higher rate and extent of silymarin release in dissolution studies. The percent hemolysis for SPY was significantly less than silymarin. As a result, SPY can be concluded to be non-toxic and biocompatible for *in vivo* administration. SPY significantly inhibited hypotonic solution-induced hemolysis in a dose-dependent manner. In acute oral toxicity, no treatment-related death or toxic signs were observed. The sub-acute

test observations indicated that there are no treatment-related changes up to the high dose level. Food consumption, body weight, organ weight, hematological parameters, biochemical parameters and histopathological examination revealed no abnormalities. **Conclusion:** The study shows that SPY is a promising and viable strategy for improving the delivery of silymarin.

Keyword: Silymarin phytosome, Hemolysis, Acute and Sub-acute toxicity, Toxicological evaluation.

Correspondence

Prof. Dr. Umesh Kumar Patil

Department of Pharmaceutical Sciences, Dr. Harisingh Gour Vishwavidyalaya (A Central University), Sagar-470001, Madhya Pradesh, INDIA.

Email id: umeshpatil29@gmail.com

DOI: 10.5530/ijpi.2022.3.52

INTRODUCTION

Silymarin (SL) is a milk thistle extract derived from *Silybum marianum* (L.) Gaertn that contains a variety of flavonolignans. The active fraction of SL consists prominently of silibinin (isoform A & B), isosilibinin (isoform A & B), silicristin, silidianin and taxifolin. SL has been shown to possess pharmacological properties like hepatoprotective, anti-inflammatory, cardioprotective, antidiabetic, hypolipidemic, anticancer and anti-viral.¹ Hepatoprotective properties of SL are widely reported and have limitation with respect to water solubility (very hydrophobic and non-ionizable chemical structure), oral absorption and rapid metabolism. Silybin is poorly absorbed in the stomach after oral administration due to its low absorption efficiency, with an absolute oral bioavailability of 0.95%.²

In the current era of novel drug delivery approaches, SL-based formulations with greater stability, solubility, increased bioavailability, and competent medicinal performances are constantly expanding. However, unintended features raise difficulties in the formulation and design of drug delivery systems, as poor water solubility of the active components affects the bioavailability.³ Nevertheless, researchers now use a range of solubilization strategies to entrap weakly water-soluble active plant constituents like SL in aqueous nano-vehicles.⁴ An effective vesicular drug delivery system allows flavonoids to be passively absorbed from the intestine into the lymphatic and blood circulation, significantly increasing their bioavailability. As a result, innovative techniques have been used to develop SL-based formulations, which have been demonstrated to improve therapeutic efficacy against a variety of disorders.⁵

The majority of formulation strategies include complexation with cyclodextrin or phospholipid (PL) complexation, biocompatible polymer-stabilized solid dispersions, micro- and nanoemulsions, lipid-based delivery systems, biodegradable polymeric NPs, and inorganic nanomaterials. PL-based complexes (phytosomes) have recently been introduced as cosmetics, antibiotics, medicinal preparations, and food-grade delivery systems for the delivery of low soluble and low bioavailable compounds, making them applicable in development of the new drug and formulations.⁶⁻⁸

In recent years, vesicular drug delivery systems such as controlled and targeted drug delivery systems have been employed to deliver drugs with improved pharmacokinetics and pharmacodynamics and also lower toxicities than the parent drugs.⁹ Phytosomes have been employed as a promising carrier for a variety of drugs and phytoconstituents, offering benefits such as prolonged circulation and reduced toxicity.⁹ Vesicular systems have the potential for systemic toxicity since phytosomes can increase bioavailability of encapsulated therapeutic agents through the gastrointestinal tract while lowering dose.⁶

SL has very low acute, sub-acute, and chronic toxicity (>1.5g/day), as its pharmacokinetics are poor in terms of absorption, fast metabolism, and limited oral bioavailability.¹⁰⁻¹¹ However, it is vital to investigate the toxicity profile of a newly prepared formulation, because the probably enhanced bioavailability and potentially resulting in toxicity. Toxicity studies aid in determining the maximum safe dose of new formulations. The acute toxicity as per OECD 423 is determined by administering a single dose in order to determine general behavior and the LD50, or

median lethal dose. While, sub-acute toxicity study uses daily dose, starting at around the expected therapeutic level. In chronic experiments, two species, one rodent and one non-rodent, are dosed daily for six months and observed for signs of toxicity.¹²

There have been reports on the formulation and development of phytosomes containing SL, but the lack of toxicity information restricts their further use. *In vivo* studies for phytosome toxicological evaluation are critical as the novel systems are extremely complex, and their interactions with biological systems may result in modified pharmacokinetic profile, metabolism patterns, bio-distribution, clearance as well as novel pharmacodynamics responses, all of which provide useful information for determining health hazards in humans.¹³

According to the USFDA, even if any changes are made to the formulation's composition, chemical modification of the substance or in the formulation can result in a new toxicity, hence preclinical data may be required.¹⁴ The Department of Biotechnology and the Indian Society of Nanomedicine collaborated to develop standards for evaluating nanopharmaceuticals in India. Toxicological studies for the innovative formulation should follow the guidelines in appendix III, schedule Y of pharmaceuticals and cosmetic rules 194 according to the guideline.¹⁵

As a result, an approach is made to prepare and evaluate SL as a PL complex in order to overcome pharmacokinetic limitations and access the formulation's toxicological profile.

MATERIALS AND METHODS

Materials

SL was purchased from Otto Chemie Pvt Ltd, and Phospholipon® 90H (HSPC) was received as a gift sample from Lipoid GmbH Germany. Phosphatidylcholine content was 97% w/w, absolute ethanol (99.9%, Merck Millipore), and methanol (99.8%, Merck Millipore), and all solvents were analytical grade or superior.

Formulation of SL-PL complex (SPC)

As per procedure prescribed by Saoji *et al.*¹⁶ PL complexes were prepared using an antisolvent precipitation approach. Briefly, in 20 ml of DCM, the required quantities of SL and HSPC were dissolved in varied molar ratios (Table 1) and refluxed using an oil bath. The reaction was regulated and maintained at varied temperatures of 40, 50, or 60±2°C for 4hr. The mixture was filtered and concentrated to 5-10 ml and hexane (20 ml) was carefully added with constant stirring. The precipitate formed was filtered, collected, and stored in vacuum desiccators overnight. The SPC was then transferred to an amber-colored vial that had been flushed with nitrogen. The phytosomes were dried thoroughly and precisely weighed. The percentage yield was calculated using equation (1).

$$\% \text{ Yield} = \frac{\text{Actual yield}}{\text{Theoretical yield}} \times 100 \quad \text{equation (1)}$$

Table 1: Coded levels and "Actual" values for each factor studied for SPC.

Variables	Levels		
	-1	0	+1
Independent	Real values		
PL:SL ratio (X ₁ , w:w)	0.5:1	1:1	2:1
Reaction temperature (X ₂ , °C)	40	50	60
Dependent			
Percentage CE (Y, %)			
Percentage LE (Y, %)			

Evaluation of the complexation efficiency (CE) of SPC

The CE of the SPC was determined using a method reported by C. Chi *et al.*¹⁷ As both free SL and its SPC dissolve in methanol, the original content of the SL was measured by dissolving a specific amount of the SPC in methanol and measuring the SL. The content of SL combined with PLs was determined by dissolving the same amount of SPC in chloroform and precipitating the uncombined SL because free SL was insoluble in chloroform. The precipitates were removed by filtration and the content of the SL dissolved in chloroform was measured. Therefore, the CE was calculated using equation (2).

$$\% \text{ Complexation efficiency} = \frac{\text{Content of silymarin dissolve in chloroform}}{\text{Content of silymarin dissolve in methanol}} \times 100 \quad \text{equation (2)}$$

Determination of drug content and drug loading in SPC

The drug content and drug loading in SPC was determined by dissolving precisely weighed 10 mg of complex in 10 ml of methanol. After an appropriate dilution, absorbance was determined by UV – Spectrophotometer ((Model Shimadzu 1800, Japan)) at 288 using HSPC solution as blank, and the drug content was calculated using a calibration curve.¹⁸ The drug loading was calculated using equation (3).

$$\% \text{ Drug loading} = \frac{\text{Content of silymarin in complex}}{\text{Total weight of complex taken}} \times 100 \quad \text{equation (3)}$$

Optimization of formulation by quality by design (QBD) using design of expert (DOE)

Full-factorial design

The response surface methodology combines mathematical and statistical methods for making statistical predictions based on fitting a polynomial equation to a set of experimental data. It has been used in studies that investigate complex multivariable systems and analyze the interaction of independent variables (factors) and their effects on dependent variables (responses).¹⁹ The formulations were optimized by DoE using response surface three level factorial randomized quadratic design and DoE were constructed with the help of design expert-10 (Stat-Ease Inc., MN, and Version10.0.1.0) software. A full factorial design (2 factor 3 level factorial design [3²]) was used to investigate the overall impact of individual independent variables, such as SL: PL ratio (X₁, w: w) and temperature (X₂, °C), on the percentage complexation and loading efficiency (LE) of SL. The two independent variables (X₁ and X₂) were coded as 1 (low), 0 (middle), and +1 (upper) at three levels, resulting in 3² factorial design with nine alternative arrangements. The dependent variables were percentage complexation and LE. All nine feasible combinations of the selected variables were used in the experimental trials. The equation 4 and 5 were used to measure the response using a mathematical model that included coefficient effects, interactions, and polynomial terms.

For complexation efficiency.

$$Y = a_0 + a_1X_1 + a_2X_2 + a_3X_1X_2 - a_4X_1^2 + a_5X_2^2 \quad \text{equation (4)}$$

For drug loading

$$Y = c_0 - c_1X_1 - c_2X_2 - c_3X_1X_2 - c_4X_1^2 - a_5X_2^2 \quad \text{equation (5)}$$

For CE and drug loading of SL, where Y is the dependent variable, while a and c are the coefficients of the independent variable X. The primary effects (X₁ and X₂) show the combined influence of both components as they change from low to high levels independently. When two factors are altered at the same time, the interaction term (X₁X₂) illustrates how the response changes. The non-linearity is described by the polynomial

terms (X12 and X22). Table 1 shows the design levels and actual values of the independent variables.

Physicochemical characterization

FTIR spectroscopy

ATR Infrared spectroscopy Bruker was used to record FTIR spectra of HSPC, pure SL, a physical mixing of HSPC and SL, and SPC as comparisons.

Differential scanning calorimetry (DSC)

The DSC of HSPC, pure SL, physical mixture of HSPC and SL, and SPC was carried out with DSC 200 F3, Netzsch, German using the standard aluminum pan heated at the speed of 10°C/minute from 40°C to 250°C in the atmosphere of pure nitrogen.

Powder X-ray diffraction (PXRD)

X-ray diffractometer (D8 Focus, Bruker, Germany) coupled with a Cu K source of radiation was used to measure the PXRD patterns of HSPC, pure SL, physical mixing of HSPC and SL, and SPC.

¹H-NMR Spectroscopy

¹H-NMR Spectroscopy of pure SL, HSPC, and SPC were studied using AVANCE III500, Bruker, German with Varian (Chemagnetics) QR T3 HFX 2.0 mm probe at 303 K experimental temperature and results of each were compared. Pure SL was dissolved in DMSO-d₆, while HSPC, and SPC were dissolved in CDCl₃, and spectra obtained at 500 MHz with tetramethylsilane (TMS) as an internal standard.

Preparation of SPY Vesicles

The thin layer method was used to prepare phytosome vesicles using a rotary evaporator. In a 250 ml round bottom flask, 10 mg of optimized SPC (ratio 1:1) was dissolved in 10 ml anhydrous ethanol. The flask was connected to a rotating evaporator and rotated at 180 rpm. To get a film on the flask wall, the solvent was evaporated at 40±2°C under reduced pressure. The cast film was dispersed in phosphate buffer saline (PBS, pH 7.4). The lipid swelled and peeled away from the wall of round bottom flask forming vesicles, after being hydrated for around 2h. Finally, the phytosomal suspension was sonicated in a bath sonicator for 4 min. Prior to characterization, SPY suspension was maintained in the refrigerator for maximum 24hr to ensure optimal stability.

Determination of particle size, polydispersity index (PDI) and surface zeta potential

The particle size and PDI of the SPY were determined by dynamic light scattering using Zetasizer instrument (Malvern Zetasizer, United Kingdom) at a fixed angle of 90° at 25±2°C. Size measurements were performed in triplicate using the 1:100 (v/v) dilutions of the phytosome in distilled water. The surface charge potential of prepared SPY was measured by using the same instrument at 25±2°C in deionized water.

Morphology of Phytosome Vesicles

The shape of SPY vesicles was observed visually with TEM. The sample was placed over the grid and allowed to stand for 1 min. A filter paper was used to clear any remaining droplets on the grid. The grid was left for 24h and the films were then viewed on a transmission electron microscope and photographed.

Entrapment Efficiency of phytosome

The proportion of encapsulated SL was determined by centrifuging a 10 ml of SPY formulation at 15000xg for 60 min at room temperature. The supernatant was taken and dissolved in methanol to disrupt the vesicles and appropriate dilution was made to measure the SL content using UV spectrophotometry at 288 nm. Entrapment efficiency (EE) was calculated by the equation (6).²⁰

$$\% EE = \frac{\text{Total silymarin in suspension} - \text{silymarin concentration in Supernatant}}{\text{Total silymarin in suspension}} \times 100 \quad \text{equation (6)}$$

Apparent water solubility

The apparent solubility was determined by adding excess of drug, physical mixture and complex to 5 ml of water in sealed glass containers at room temperature.²¹ To remove excessive drug or complex, the liquids were agitated for 24h then centrifuged for 20 min at 1,000 rpm. The supernatant was filtered through a membrane filter (0.45µm), and 1 ml filtrate was diluted with 9 ml of distilled water prior to measure absorbance at 288 nm using UV spectrophotometer.

Apparent octanol–water partition coefficient

The partition coefficient was calculated using the approach described by Yanyu *et al.*²¹ and Zeng *et al.*²² with some modifications. The SPC was dissolved in n-octanol to produce a concentration of 200 g/ml. 5 ml of the solution was combined with 45 ml of hydrochloric acid (0.1 M, pH 1.2), distilled water (pH 5.6), or an n-octanol-saturated phosphate buffer with pH values of 6.8, 7.4, and 7.4 individually in a conical flask. To achieve saturation and equilibrium, the prepared sample was shaken for 24h at 300 rpm at 37°C in a conical flask. The sample was then separated into an octanol and aqueous phase using a separating funnel. One ml of the octanol phase containing the SPC was taken and diluted with 9 ml of methanol, followed by a spectrophotometer measurement at 288nm to determine the drug concentration. The apparent octanol–water partition coefficient (log P) was calculated according to equation (7) and (8).

$$C_w = (C_o - C)V_o / V_w \quad \text{equation (7)}$$

$$\log P = C_o / C_w \quad \text{equation (8)}$$

Where C_o and C represent the drug concentration (µg/ml) in the aqueous phase before and after equilibrium, respectively, and C_w represents the drug concentration in the octanol phase after equilibrium. V_o and V_w represent the volume (ml) of octanol and aqueous phase in the equilibrated solution, respectively.

Stability studies

Stability study was performed to assess the change in drug content, LE, and CE for SPC and entrapment efficiency and physical appearance for the optimized phytosome. Prepared SPC and SPY formulations were kept sealed in glass vials and stored at a temperature 4 ± 0.5°C and 25±0.5°C for a period of 3 months as per ICH guidelines.²³ Samples were withdrawn at 1, 2 and 3 months in triplicate manner. In addition, the drug content, LE, and CE for SPC and entrapment efficiency for the optimized SPY were measured as described above.

Functional Characterization

In vitro Drug Release Studies

The *in vitro* dissolution phenomenon of pure SL, and SPC was analyzed using a dialysis method reported earlier with some modifications.²⁴⁻²⁵ The membrane was washed according to the manufacturer guidelines. To ensure uniform distribution, 2 ml of SPC (2 mg/ml) or 4 mg SL were added to a dialysis membrane bag (MWCO-3500), which was then immersed in 900 ml of PBS (0.01 M, pH 7.4) and continuously stirred with a magnetic stirrer at 120 rpm. The temperature of the entire assembly was maintained at 37±1°C. At specified time intervals (0, 10, 20, 30, 40, 50, and 60... n min), 1 ml aliquots of the media outside the dialysis bag were obtained for UV analysis, and the entire medium was replaced with the same volume of fresh PBS (0.01 M, pH 7.4).

The absorbance of the sample was measured by spectrophotometry at 288 nm and the amount of drug was obtained through the calibration curve. The percentage cumulative release was calculated as per equation (9).

$$\% \text{ Cumulative drug released} = \frac{\text{Cumulative amount of silymarin obtained at time in phytosome}}{\text{Total amount of silymarin}} \times 100 \quad \text{equation (9)}$$

In vitro hemolysis study

An important preclinical test is the *in vitro* examination of phytosome compatibility with red blood cells (RBC). By measuring the optical absorbance given by the liberated haemoglobin in the supernatant, the extent of hemolysis for the controls and exposed samples was indirectly measured. *In vitro* hemolysis study was carried out using procedure reported by Nuruki *et al.*²⁶ Hemolysis of phytosomal formulations was studied at high (1000 µg/ml), medium (100 µg/ml), and low (10 µg/ml) concentrations, using pure SL as a control. To obtain clear cells, blood from a healthy volunteer was centrifuged at 1500g for 20 min and rinsed three times with normal saline. To achieve a 50% hematocrit, normal saline was added to the cells. As a negative control, a 3 ml normal saline solution containing 100 µl cell suspension was employed (0% hemolysis). Meanwhile, 100 µl cells were taken in test tube and diluted with 3 ml double distilled deionized water was used as positive control (100% hemolysis), as RBCs lyse in a hypotonic medium. After that, phytosomal preparation at different concentrations were added to different tubes containing cell suspension. The samples were incubated at 37±2°C for 3hr in a shaker. After 3h, the samples were centrifuged at 1500g for 15 min and then checked the absorbance at 540 nm by UV/VIS spectrometer. A % hemolysis ratio less than 5 % was regarded nontoxic. Percent hemolysis was calculated as per equation (10).

$$\text{Hemolysis (\%)} = \frac{\text{Absorbance of samples} - \text{Absorbance of negative controls}}{\text{Absorbance of positive control} - \text{Absorbance of negative control}} \times 100 \quad \text{equation (10)}$$

In vitro membrane stabilizing activity

The method developed by Shinde *et al.* was used to investigate the membrane stabilizing activity.²⁷ Briefly, 5 ml of the whole blood from healthy human volunteers was collected in a tube containing dipotassium salt of EDTA (2.2 mg/ml of blood). The blood was centrifuged to collect blood cells, and then washed three times with isotonic solution (154 mM NaCl) in 10 mM sodium phosphate buffer (pH 7.4) using the same volume as supernatant through centrifugation (10 min at 3000 g). Finally, it was re-suspended in the equal volume of this isotonic buffer solution. 0.5 ml of the suspension was combined with 5 ml of hypotonic solution (50 mM NaCl) in 10 mM sodium phosphate buffered saline (pH 7.4) with varying concentrations of SL, SPY, or acetylsalicylic acid as a reference. The control sample had 0.5 ml of erythrocytes mixed with hypotonic-buffered saline alone. The mixture was incubated for 10 min at room temperature, centrifuged for 10 min at 3000 g and the optical density (OD) of the supernatant was measured at 540 nm by using a UV-visible spectrophotometer. The percentage inhibition of hemolysis was calculated using equation (11).

$$\% \text{ inhibition of hemolysis} = \left[1 - \frac{\text{OD}_2 - \text{OD}_1}{\text{OD}_3 - \text{OD}_1} \right] \times 100 \quad \text{equation (11)}$$

Where OD1 is test sample in isotonic solution, OD2 is test sample in hypotonic solution, OD3 is control sample in hypotonic solution

Experimental animals

Albino wistar rats of either sex were used for the acute and sub-acute oral toxicity tests. Nine rats (females) were used in an acute oral toxicity test, whereas 30 rats (15 males and 15 females) used in sub-acute oral toxicity test (the repeated dose 28 day). The toxicity tests were carried out according to Organization for Economic Cooperation and Development (OECD) test guideline, i.e., OECD Guideline 423 for the acute oral toxicity test²⁸ and OECD Guideline 407 for the sub-acute oral toxicity test.²⁹ The rats were obtained from the Animal house after approval of protocol by the Institutional Animal Ethical Committee (IAEC) (Ethics No. 379/CPCSEA/IAEC-2018-II/019) of Department of Pharmaceutical Sciences, Dr. Harisingh Gour Vishwavidyalaya, Sagar Madhya Pradesh, India. Wistar rats (8-10 weeks) weigh between 180±15 g were used. The female rats were nulliparous and non-pregnant. The rats were given standard rat pellets and water *ad libitum*. They were acclimatized to laboratory conditions for 7 days before the experiments and housed in groups of three for acute oral toxicity and in groups of five for sub-acute oral toxicity. The rats were maintained at a room temperature of 22 ± 2°C, with a 12hr light/dark cycle. The endpoint of all rats considered when around 20% of body weight loss has been shown.

Acute oral toxicity

SPY was administered to the female rats under overnight fasting by using oral gavage in a volume of 10 ml/kg body weight.

Nine female albino wistar rats were divided into 3 groups of 3 rats in each group for SPY as mentioned previously.³⁰ The starting dose of SPY at 50 mg/kg according to body weight administered to the group 1. All rats were observed for behavioral changes, toxicity and mortality after treatment for the first 4h, then over a period of 48 hr. Group 2 was administered successively at 48-h intervals with the next higher dose 2000 mg/kg body weight of SPY when there were no signs of toxicity or mortality showed in group 1. Separately, group 3 treated with vehicle as negative control group according to the OECD guideline. All animals observed at every 30 min up to 4hr and then up to 24hr after administration and then once daily for 14 days. This observation was done to access the onset of toxic symptoms including changes in skin and fur, eyes and mucous membranes and behavioral changes were recorded. Furthermore, animal were also observed for sign convulsions, tremors, diarrhea, salivation, lethargy, sleep, coma and mortality. The food consumption and water intake recorded daily. The body weights of animals was recorded weekly. The percentage of body weight change calculated according to equation (12).

$$\% \text{ Body weight change} = \frac{\text{Body weight at the end of each week} - \text{Initial body weight}}{\text{Initial body weight}} \times 100 \quad \text{equation (12)}$$

Sub-acute oral toxicity

Albino wistar rats were randomly divided into six groups of 6 rats each (*n*=6/group, 3 males and 3 females) for SPY.³⁰ Four groups were administered daily with SPY at different concentration and two groups administered with the vehicle by using oral gavage. Group 1 received vehicle and served as control. Groups 2, 3 and 4 received doses of SPY at 500, 1000 and 1500 mg/kg body weight, respectively. The 5th and 6th groups namely recovery groups used to study recovery from toxic effects of the SPY and given the vehicle and the top dose of SPY 1500 mg/kg body weight, respectively. The administration was done orally once daily for 28 days. The recovery groups were followed-up with the observations for the next 14 days without treatment.

Hematology and serum biochemistry

At the end of each experiment, a blood sample (2ml) was collected in different tubes via the retro-orbital plexus under mild anesthesia and used for hematological parameters such as hemoglobin (HGB), white blood cell (WBC), neutrophil, lymphocyte, monocyte, eosinophil, and basophil and biochemical parameters [Urea, Creatinine, Albumin, Globulin, Total bilirubin, Conjugate Bilirubin, Alkaline phosphatase (ALP), Alanine transaminase (ALT) and Aspartate aminotransferase (AST)].

Histopathological observation

Necropsy was done in both groups of animals on day 15 and 29 respectively, and for the recovery groups, on day 43. After the blood collection, rats were sacrificed by cervical dislocation, and the vital organs (Brain, heart, liver, kidney, spleen and lung) removed. The organs were cleaned of fat and blotted with clean tissue paper, and then weighed on balance. The relative organ's weight (ROW) were calculated and recorded in proportion to the body weight according to equation (13).

$$\text{Relative organ's weight} = \frac{\text{Absolute organ weight}}{\text{Body weight at sacrifice}} \times 100 \quad \text{equation (13)}$$

Samples from the vital organs of both studies were processed for histopathological evaluation. They were fixed in 10% buffered formalin, processed and embedded in paraffin wax. Paraffin sections (5 μ m) was prepared on glass slides and stained with hematoxylin and eosin. An experienced pathologist conducted the analysis of all blinded slides. The slides were examined under a light microscope (Nikon E50i, Nikon Corporation, Japan).

Statistical Analysis

Results were expressed as a mean \pm standard deviation (SD). The differences between acute and sub-acute toxicity groups determined by one-way analysis of variance (ANOVA) followed by Tukey multiple comparison test, and Student t test for recovery groups comparisons using Graph pad prism software 5.1. Differences were considered significant at $p < 0.05$.

RESULT AND DISCUSSION

Preparation and Characterization of SPC

SPC was prepared by antisolvent precipitation technique. Numerous constraints are critical for formation of SPC including ratio between SL and PL, solvents, reaction time, and temperature. The problem with SL is that it is partially soluble in DCM, and forms precipitate in reaction mixture. In the present study, when the SPC is formed during the reaction, insoluble SL get solubilize in DCM as complex and also help to indicate the reaction end point. The molar ratio between SL and PL plays an important role in the formation of complex because it affect the yield of the complex. The different molar ratio, drug content, drug loading and CE are tabulated in Table 2. The percentage yield (38.18 \pm 0.70 to 40.59 \pm 0.41 %) was obtained with the different molar ratio. The SL content, drug loading and CE in the SPC with the different molar ratio at 50°C was found to be 79.86 \pm 0.72 to 84.40 \pm 0.73%, 63.98 \pm 0.74 to 70.72 \pm 1.49 % and 80.11 \pm 0.18 to 83.78 \pm 1.03% respectively. When SPC form, the hydrophilic head group of HSPC is directed toward the hydrophilic areas of SL, allowing PL complexes to be a central part in which the PLs head group is attached, but fatty acid chains are free to move and encapsulate the polar part of complexes to form a lipophilic surface.⁶

Table 2: Percentage Yield, Drug content, and CE of SPC.

HSPC : SL Ratio	Yield	Drug content	Drug Loading	Complexation efficiency
0.5:1	38.18 \pm 0.7065	82.90 \pm 0.72	67.43 \pm 0.29	81.34 \pm 0.37
1:1	40.59 \pm 0.4079	84.40 \pm 0.73	70.72 \pm 1.49	83.78 \pm 1.03
2:1	37.83 \pm 0.2946	79.86 \pm 0.72	63.98 \pm 0.74	80.11 \pm 0.18

Data were expressed as mean \pm SEM ($n=3$).

Table 3: Full factorial design experimental runs together with respectively obtained % CE and LE for SPC.

Experimental trials	X1	X2	% CE	% LE
1	1	1	83.10 \pm 0.05	62.63 \pm 0.58
2	-1	0	77.01 \pm 0.04	66.45 \pm 0.50
3	-1	-1	76.29 \pm 0.11	65.77 \pm 1.32
4	0	1	84.27 \pm 0.32	70.12 \pm 1.49
5	0	0	80.52 \pm 0.39	71.50 \pm 1.79
6	0	-1	78.28 \pm 0.15	70.75 \pm 0.44
7	1	-1	75.62 \pm 0.21	62.79 \pm 0.77
8	-1	1	79.97 \pm 0.06	66.30 \pm 0.65
9	1	0	78.45 \pm 0.03	62.78 \pm 0.58

Data were expressed as mean \pm SEM ($n=3$).

Full-factorial design

The results of the CE and LE from the experimental trials carried out using a 3² full factorial design are shown in Table 3. The results indicated that the CE and LE was significantly influenced by both the variables studied, i.e. SL: PL ratio (X1, w:w) and the reaction temperature (X2, °C). For the nine experimental batches examined (with different combination of variables), the observed extent of CE and LE ranged between 75-84% and 62-71% respectively.

X1X2 is measure of the effect of interaction (represents the change in the response when both the factors are simultaneously changed), the polynomial terms or the second-order quadratic terms (X2 1 and X2 2) are incorporated to examine nonlinearity. These data were used to construct a quadratic model relating the extent of CE and LE to the tested variables representing the quantitative effect of the independent variables (X1, X2). The resulting polynomial equation (14) for CE and equation (15) for LE was used to draw conclusions based on the magnitude of the coefficient, as well as the sign (+, or -) associated with it.

$$\text{CE (Y}_1\text{)} = 80.40 + 0.65 \times X_1 + 2.85 \times X_2 + 0.95 \times X_1X_2 - 2.61 \times X_1^2 + 0.92 \times X_2^2 \quad \text{equation(14)}$$

$$\text{Drug loading (Y}_2\text{)} = 71.13 - 1.72 \times X_1 - 0.043 \times X_2 - 0.17 \times X_1X_2 - 6.33 \times X_1^2 - 0.51 \times X_2^2 \quad \text{equation(15)}$$

The estimated coefficient value of a_0 , a_1 , and a_2 , were found statistically significant whereas a_3 , a_4 and a_5 were found to be not significant statistically for CE. Similarly, the estimated coefficient value of c_0 , c_1 , and c_4 for LE were found to be statistically significant, while c_2 , c_3 and c_5 were not significant. These observations, coupled with the observed value of the correlation coefficient for CE ($R^2=0.9986$) and LE ($R^2=0.9943$), lead us to conclude that this was the best representative model for the study. The positive sign associated with coefficients (a_1 and a_2) indicated a positive correlation between the studied variables and the complexation

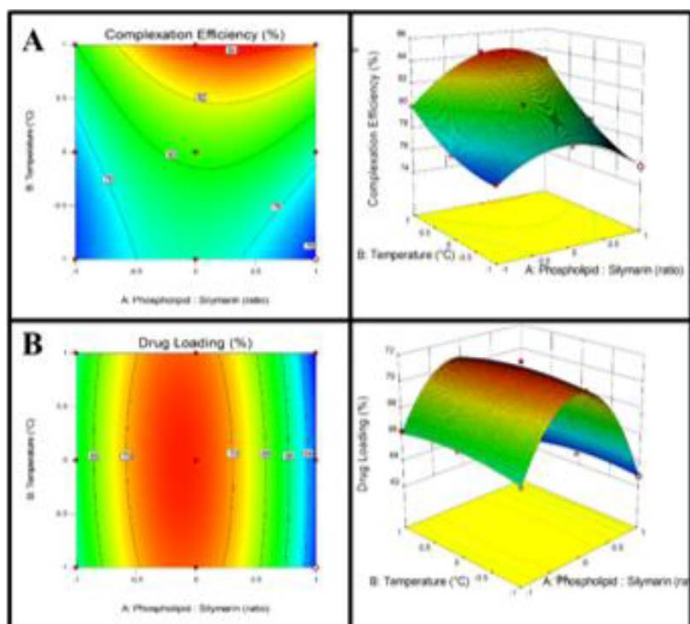


Figure 1: The response surface plot and contour plots (A) Complexation efficiency (Y_1 , %) (B) Loading efficiency (Y_2 , %) as a function of the ratio of SL and Phospholipon® 90H (X_1 , w:w), and the reaction temperature (X_2 , °C).

efficiency. The negative sign associated with coefficients (c_1 and c_2) indicated a negative correlation between the studied variables and LE. The influence of the studied variables on the CE as well as LE is also shown in the form of response surface and contour plot (Figure 1). Based on these observations, along with calculations from the developed quadratic model, the optimal values for the studied variables, i.e. drug: PL ratio (X_1 , w:w) and the reaction temperature (X_2 , °C) were found to be 1:1, and 60 °C, respectively.³¹ The CE increased as the amount of phospholipid increased. When the ratio of SL to PL was 1:1 and the temperature was 60°C, the CE of SL was at its peak. Furthermore, we found that temperature changes had a significant impact on the CE, implying that temperature is directly proportional to complexation. Chi *et al.* reported a silybin phospholipid complex with the highest CE at a ratio of 1:1, but that temperature has the least effect on CE.¹⁷

Validation of the optimized model

An additional batch of SPC was prepared in order to validate the model using the optimized values of the variables. A comparison between the predicted (theoretical) percentage complexation and LE of the complex obtained from the developed model and the actual percentage complexation and LE achieved from the prepared formulation was carried out. The model-predicted value for the average percentage complexation and LE of SL in the optimized SPC was 84.27% and 70.12% respectively, whereas the actual percentage complexation and LE of SL in prepared batch was found to be $85.50 \pm 0.44\%$ and $70.87 \pm 0.75\%$ respectively, indicating both applicability, and validity of the developed model. The bias (%), calculated using the Equation (16), was also found to be lower than 3.48% (-1.45%), indicating the relative robustness of the model.

$$\text{Bias \%} = \frac{\text{Predicted value} - \text{observed value}}{\text{Predicted value}} \times 100 \quad \text{equation (16).}$$

PHYSICOCHEMICAL CHARACTERIZATION

Fourier transform infrared spectroscopy (FTIR)

The molecular interactions between the formulation constituents were analyzed by obtaining the infrared scans on a FTIR spectrophotometer. The peaks and pattern of FTIR spectra confirmed the presence of chemical interactions between SL and PL as seen on Figure 2. The FTIR spectrum of HSPC (Figure 2A) revealed the characteristic 2913.54 and 2850 cm^{-1} (C-H), 1731.41 cm^{-1} (C=O stretching), 1254.27 cm^{-1} (P=O stretching), 1086.40 cm^{-1} (P-O-C stretching) and $-\text{N}+(\text{CH}_3)_3$ stretching at 961.85 cm^{-1} . SL IR Spectra (Figure 2B) exhibited bands at 3642.27 cm^{-1} (OH), 2346.85 cm^{-1} (CH) and 1741.71 cm^{-1} (C = O). These peaks were suppressed in the SPC IR Spectra and present with weaker intensity. Additionally, the peak presented by HSPC at 1254.27 cm^{-1} due to the P = O group was obscure in the spectrum of SPC (Figure 2D). This indicates the interaction between SL and PL. The complex is being formed due to presence of P = O present in PL. The IR spectra of the physical mixture (Figure 2C) revealed almost all bands of SL, and HSPC, proposing that there was no chemical interaction in the physical mixture. Furthermore, the stretching vibration of free -O-H (3642.27 cm^{-1}) in SL become broadened and also peak intensity was increased, this indicates the formation of a hydrogen bond between the SL and HSPC. Overall, from the IR analysis we can assume that there was no new bond formation between SL and HSPC, but the change in spectra may be due to weak intermolecular interaction, such as hydrogen bonding or vander waals forces.¹⁷

Differential scanning calorimetry (DSC)

DSC is used to assess the crystallinity and thermal behavior of the lipid material. The objective of DSC study is to identify the crystalline form of SL in complex and to compare its thermal behavior with the same. The

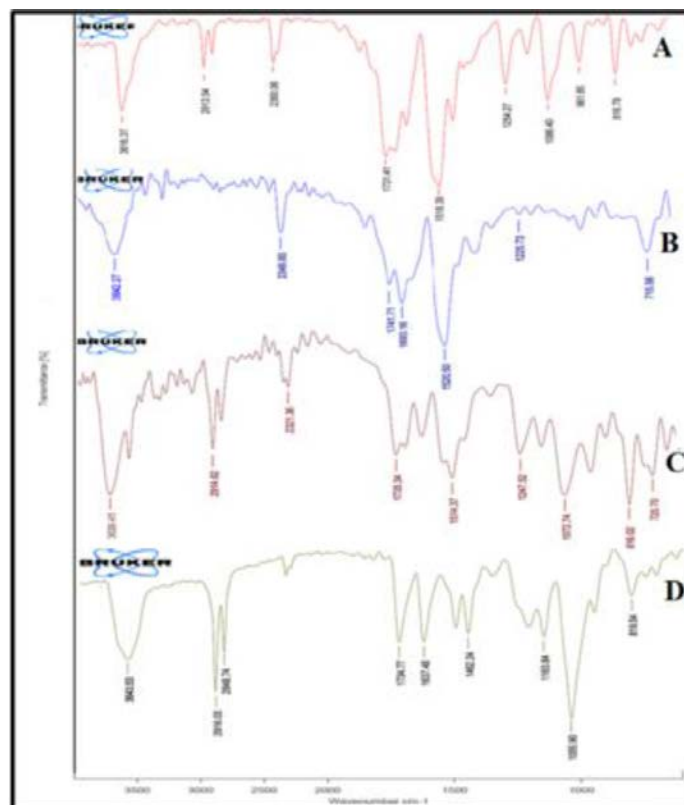


Figure 2: Fourier transform infrared spectra of HSPC (A), SL (B), Physical mixture (C) and SPC (D).

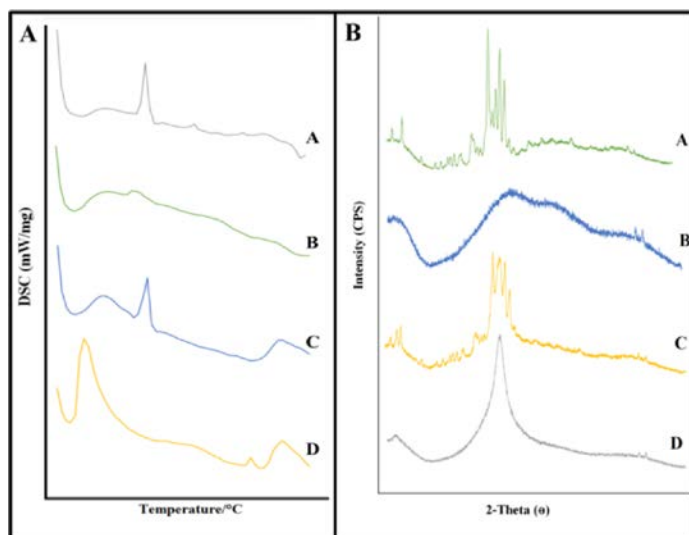


Figure 3: DSC and XRD Pattern. (A) DSC of HSPC (A), SL (B), Physical mixture (C) and SPC (D). (B) XRD of HSPC (A), SL (B), Physical mixture (C) and SPC (D).

thermal behavior of HSPC powder (Figure 3A/A) was characterized by a number of endothermic events were observed. At 125°C, a significant endothermic peak was seen, which corresponded to side chain partial melting and therefore the transition of phosphatidylcholine to the liquid crystalline state. Transitions were also seen at 145, 160, and 180°C, indicating more phase transitions. Finally, a small peak was observed at 233–235°C, where the capillary melting of the HSPC was expected. SL (Figure 3A/B) had endothermic peaks at 106.44°C, 135.41°C, and 227.16°C, which were not prominent because SM is a multicomponent mixture. The physical mixture of SL and HSPC (Figure 3A/C) has exothermic peak at 226.36°C and 123.78°C which corresponds to the peak of both components respectively. In the thermogram of SPC (Figure 3A/D), the peaks of SL and PL all disappeared and curve shown HSPC peak shifted little to a higher temperature. It was hypothesized that increase in temperature leads to melt PL that allow SL to dissolve in the PLs forming PLs complex due to melt out phenomenon. As a result of this phenomenon, it's assumed that SL interacts with HSPC, and that the interactions are caused by weak intermolecular interactions, van der Waals forces, or hydrogen bonding, either alone or in combination. This could also mean that the aromatic ring of SL is responsible for some hydrophobic interactions in the SL-HSPC interaction. Actually, the interaction of SL with the polar head group of HSPC molecules leads two long fatty acid chain tails of HSPC to turn freely and enwrap the polar head of HSPC containing the SL molecule, thus SL could be molecularly dispersed in HSPC.^{7,32}

Powder X-ray diffraction

XRD is used to evaluate the physical state of SL in the SPC. The XRD patterns are shown in Figure 3. HSPC's XRD diffractogram (Figure 3B/A) exhibits partial sharp crystalline peaks, which are typical of a molecular compound with some crystallinity, whereas pure SL (Figure 3B/B) showed multiple sharp distinctive peaks, showing that SL was in the crystalline form. The strength of the diffraction peaks in the physical mixture's XRD diffractogram (Figure 3B/C) decreased slightly, but some typical crystalline patterns remained, showing that SL was retained in their physical mixture. On the other hand, the characteristic crystalline peaks disappeared in the diffractogram of the SPC (Figure 3B/D) indicating the conversion of the crystalline form of SL into the amorphous form, suggesting that SL existing in the HSPC matrix was either molecularly dispersed or in the amorphous form. This result

demonstrated that the some interactions have been happened between SL and HSPC in the complex. These findings suggested that after electron transfer, SL was attached to the polar end of the PL, resulting in a highly scattered state in which the crystal characteristic of SL was obscured. The SL-PL combination has a larger free energy, molecular momentum, and dissolving ability than SL due to its amorphous state.³³

¹H-NMR Spectroscopy

SL is made up of flavonolignans with virtually identical ¹H-NMR spectra, making it difficult to distinguish them as independent components such taxifolin, silycristin, silydianin, silybin A, silybin B, and isosilybin. However, the overall flavonolignans mixture has a comparable signal in ¹H NMR, which simplifies the complex patterns of SL, allowing the SPC to be analyzed using a ¹H-NMR fingerprint.³⁴

The ¹H-NMR spectra of HSPC, SL, and SPC were shown in Figure 4. The ¹H-NMR spectra of SL (Figure 4A) have aromatic hydroxyl group's proton signals at OH-7 (12.00 ppm), OH-5 (11.00 ppm), OH-4 (9.00 ppm), OH-3 (5.83 ppm) and aliphatic hydroxyl group's proton signals at OH-9 (3.94 ppm). In the ¹H-NMR spectra of HSPC (Figure 4B), the characteristic signals of -N(CH₃)₃⁺ is present at 3.344 ppm and the fatty acid chains protons appear between 1.168 - 1.334 ppm. In the ¹H-NMR spectra of SPC (Figure 4C), proton signals at 12.00 ppm, 11.00 ppm, 9.00 ppm, 5.83 ppm and 3.94 ppm were absent or suppressed when compare with the spectra of SL alone. The protons of HSPC fatty acid chains between 1.168-1.334 ppm were clear with no changes, indicating that fatty acid chain were not involved in complex formation. Signals of -N(CH₃)₃⁺ in HSPC at 3.344 ppm were widened and upfielded to 2.959 ppm indicating that the PL head was involved in complex formation via intermolecular interactions. All other chemical shifts are intact. Thus, the spectral comparisons confirm the complexation of SL with the HSPC in the formation of SPC. The results of this ¹H-NMR investigation were found to be similar to Chi *et al.* study, in which silybin was employed for complexation.¹⁷

Determination of particle size, polydispersity index (PDI) and surface zeta potential

Lipid-based delivery systems are used to enhance the bioavailability of poorly-soluble lipophilic and/or hydrophilic drugs. The average particle size/diameter and the polydispersity index (PDI) are physical parameters of lipid-based systems that determine their safety, stability, efficacy, and *in vitro* and *in vivo* behavior.³⁵ Pharmacokinetics, tissue distribution, and clearance may be affected by the size of delivery systems. Hepatic absorption and accumulation, tissue diffusion, tissue extravasation, and

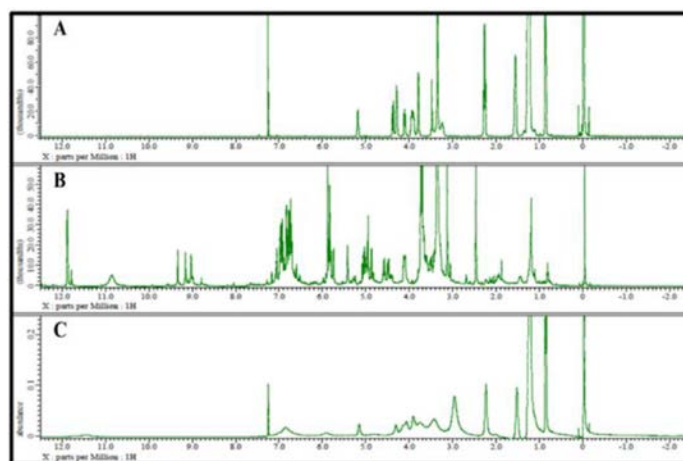


Figure 4: ¹H NMR spectra of HSPC (A), SL (B), and SPC (C).

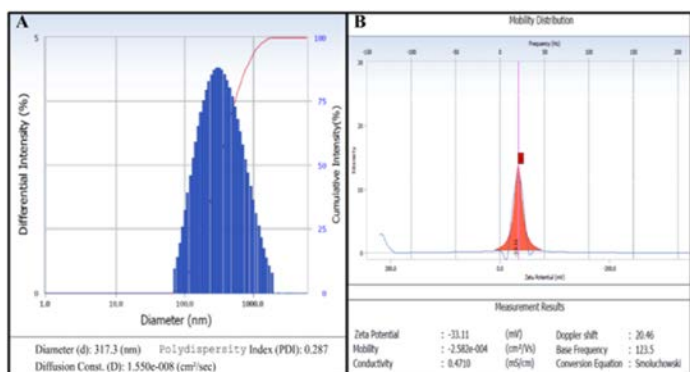


Figure 5: Particle size and zeta potential analysis. (A) Characterization of SPY by particle size analysis, showing the size-dependent distribution of the phytosomes; (B) zeta potential analysis showing the surface charge of -33.11 mV for the SPY, which corresponds with the stability of the phytosomes.

kidney excretion may all be affected by particle size.³⁶ The polydispersity index (PDI) is another important parameter that defines the spread of the particle size distribution. The PDI value may vary from 0 to 1, where PDIs less than 0.1 implies monodisperse system and the values more than 0.1 may imply polydisperse system.³⁵ Zeta potential is another important measure of stability of a colloidal system or suspension. Due to electrostatic repulsion between particles with the same charge, zeta potential values play a key role in stabilizing particle in suspension.³⁷ Figure 5 depicts the average particle size, polydispersity index (PDI), and Zeta potential. As shown in Figure 5A, optimized SPC were dispersed in aqueous medium (PBS) and self-assembled into phytosomes with a mean particle size of 317.9 ± 0.55 nm and a polydispersity index of 0.247 ± 0.03 . The low polydispersity index implies a narrow range of particle sizes and is suitable for oral administration. As demonstrated in Figure 5B, the zeta potential value (33.11 ± 0.30 mV) measured for SPY was larger than 30 mV, indicating exceptional stability. The zeta potential with range (-20 to 30 mV) was considered as a characteristic property for attraction followed by flocculation exceeding repulsion forces. The zeta potential depends on the type and composition of PLs. In SPY, the low zeta potential value was due to generation of negative charge by PL in aqueous environment with neutral pH.¹⁹ Therefore, with smaller particle size, low PDI and modest zeta potential value suggested a good physical stability for SPY.

7.6 Transmission electron microscopy (TEM)

TEM was used to study the size and the shape of the dispersed SPYs and found in range of 100-500 nm. Figure 6 shows an illustrative TEM images for SPYs in dispersed system showing characteristic spherical structures with a diameter similar to that measured using dynamic light scattering. Maryana *et al.* prepared phytosome containing SL using thin layer-hydration method for oral delivery found uniform size of phytosome in 100-200 nm range with spherical shape.³²

Entrapment efficiency of phytosome

Entrapment efficiency is an expression of the amount of drug incorporated into the phytosome and is normally defined as the percentage of drug bound to PL relative the total amount of drug.³⁸ Separation of the free drug from the phytosomal formulation is usually required to determine this parameter. The entrapment efficiency can be calculated by analyzing the drug in both the free and encapsulated drug fractions. The difference in PL to SL molarity has a considerable impact on the amount of SL incorporated in phytosomes (result of different ratio were tabulated in Table 4). The maximum encapsulation efficiency of SL in formulation

Table 4: EE of SPY at different ratios.

Lecithin: Drug Ratio	EE
0.5:1	92.32 ± 0.08
1:1	93.86 ± 0.37
2:1	92.47 ± 0.60

Data were expressed as mean \pm SEM ($n=3$).

Table 5: Solubility of SL, mixture of SL and HSPC, and SPC in distilled water.

SN	Sample	Aqueous Solubility ($\mu\text{g/mL}$)
1	SIL	16.07 ± 0.061
2	SL-PL physical mixture	33.87 ± 0.073
3	SPC	69.67 ± 0.065

Data were expressed as mean \pm SEM ($n=3$).

was found to be 93.86 ± 0.37 %. The more PL added into the formulation, the entrapment efficiency of phytosome was decrease (result of different ratio were tabulated in Table 4). These results were similar to Saputra *et al.* work where they also found that the increase in PL concentration decrease in entrapment efficiency of myricetin nano-phytosome.³⁹

Apparent water solubility

Solubility is the important parameters that effect the bioavailability of the drugs after oral administration. During oral absorption, solubility is a limiting factors that prevent absorption of drugs through the GI membrane; therefore it is important to measure and ensure that the desired amount of drug is being delivered. Water is major component in all body fluids. Therefore, all drugs that are administered in the body must display a maximum aqueous solubility for therapeutic efficiency. Accordingly, moderately insoluble compounds may exhibit unsatisfactory absorption.⁴⁰ In the present study, the solubility of SL, SL-PL mixture and SPC were evaluated in aqueous medium. Table 5 shows that the solubility of SPC ($69.67 \pm 0.065 \mu\text{g/ml}$) was significantly improved as compared with SL ($16.07 \pm 0.061 \mu\text{g/ml}$) and SL-PL mixture ($33.87 \pm 0.073 \mu\text{g/ml}$). Therefore, it can be concluded that phytosome complex technique improved the solubility of poorly water-soluble SL due to the amorphous features of the complex and the ability of PL to form micelle in aqueous solution. Qi-ping Zeng *et al.* found that SL conjugated with phospholipid have improved the solubility of SL.²²

Apparent octanol-water partition coefficient

The apparent partition coefficient, $\log P$, is a measure of hydrophilicity/lipophilicity and also an indicator for evaluating the absorbability of a compound. The biological properties such as bioaccumulation and toxicity are largely determined by $\log P$ value.⁴¹

Membrane permeability is largely dependent on partition-coefficient. Drugs having a high partition coefficient can pass through biological membranes with ease. Drugs having a $\log P$ between 1 and 2 are easily absorbed, according to various research.⁴² In the phosphate buffers with varying pH values, the $\log P$ of SL was less than 1, indicating poor permeability and absorbability. In comparison with SL, the $\log P$ values of SPC increased in various buffers as shown in Table 6. This improvement may be due to the polar groups of the drug and PL interaction and inhibition of free rotation of the bond in the drug molecule. However, the two long fatty chains of PLs did not participate in the complex reaction and were freely movable, covering the polar part of the PLs and constitute a lipophilic surface, which gives the SPC a strong fat-soluble characteristic. This promotes drug retention in the lipid membrane of cells, thereby increasing drug absorbability.²²

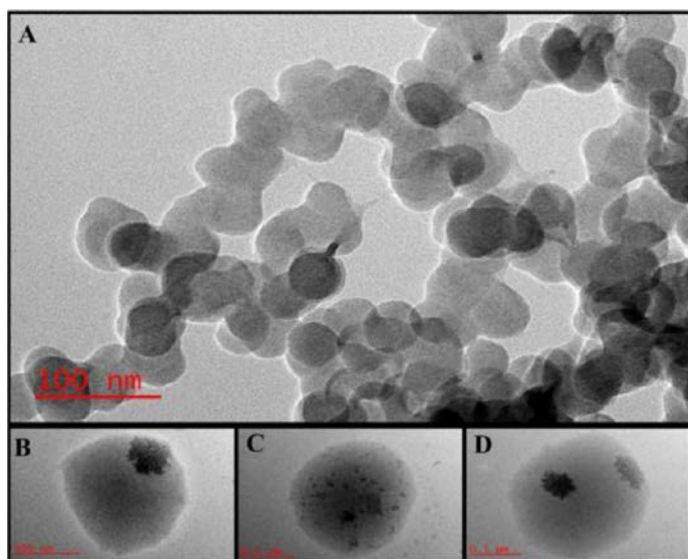


Figure 6: TEM micrographs of the optimized SPY at 10000x (A) and 20000x (B, C, D).

Table 6: Apparent octanol-water partition coefficient (Log P Value) of SL and SPC complex.

Solvent	Log P Value	
	SIL	SPY
pH 1.2 hydrochloric acid	0.8155 ± 0.02	1.706 ± 0.01
Distilled water (pH 5.6)	0.6922 ± 0.01	1.602 ± 0.01
pH 6.8 phosphate buffer	0.5070 ± 0.009	1.564 ± 0.002
pH 7.5 phosphate buffer	0.3422 ± 0.004	1.311 ± 0.004

Data were expressed as mean±SEM ($n=3$).

Stability studies

The physical appearance of SPC and phytosome formulation stored at 4°C and 24°C for 1, 2, and 3 months was evaluated. At the end of 1, 2, and 3 months, both complex and phytosome stored at 4°C and 24°C were stable. The drug content, LE, CE and physical appearance for complex and entrapment efficiency and physical appearance for phytosome as a function of temperature were also evaluated after the end of 1, 2, and 3 months. Both complex and phytosome stored at 4°C and 24°C, there is no significant change in drug content, LE, CE and physical appearance for complex and entrapment efficiency and physical appearance for phytosome at 4°C and 24°C as described in Table 7.

Functional Characterization

In vitro Drug Release Studies

For both, SPY and SL the percentage cumulative drug release study were performed in PBS (0.01 M, pH 7.4) for the 70 min and found to be 96.91 and 26.34 % respectively as shown in Figure 7. The increase in *in vitro* release of SPY was the result of improved solubility due to complex formation with PL. It was apparent that *in vitro* release of SPY showed a very rapid initial burst, and then followed by a slow drug release, while SL shows very slow release from the membrane due its poor water solubility. An initial, fast release of SPY suggest that some drug was confined on the surface of the phytosome.

In the current study, the *in vitro* release studies of SPY and SL were evaluated to a number of kinetic model using DD solver,⁴³ including zero-order, First-order, Higuchi's model, Korsmeyer-Peppas, and

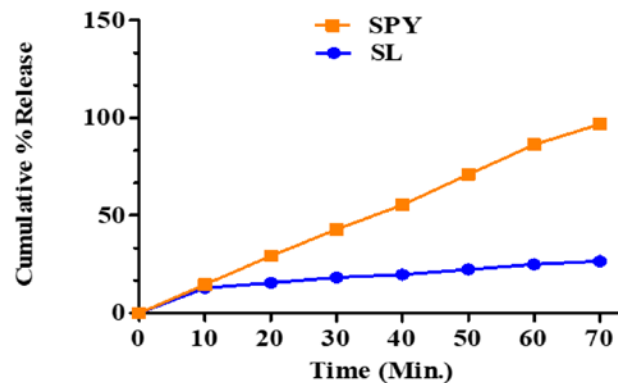


Figure 7: Release profiles of SPY in PBS (0.01 M, pH 7.4).

Hixson-Crowell model equation.⁴⁴ The data of the *in vitro* release was placed in different equations and determine the suitable kinetics model for both. The adjusted R^2 (R_{sqr_adj}), Model Selection criteria (MSC), and akaike information criterion (AIC) were used to choose the good fit model (Table 8). The R_{sqr_adj} should be as possible as near to 1, the MSC should be above 2-3, and the AIC value should be minimum (in between 30-50). SPY and SL did not fulfill the criteria of zero-order, First-order, Higuchi's model, and Hixson-Crowell model, but seems to fulfill Korsmeyer-Peppas model in term of R_{sqr_adj} , MSC, and AIC. For the Korsmeyer-Peppas model, the value of SPY and SL with R_{sqr_adj} was 0.9990 and 0.9931, MSC value of 6.16 and 3.66, and AIC value of 19.91 and 12.48, respectively. The n value ((Mt/M_∞)) of SPY and SL for Korsmeyer-Peppas kinetics were found to be 0.966 and 0.397, respectively. With n value higher than 0.89, the Korsmeyer-Peppas kinetics model for SPY suggest that the drug release was mainly determined by non-Fickian diffusion and t^{n-1} dependent which is related to super Case-II release of drug transport mechanism which is associated with stresses and state transition in hydrophilic surface of PL which swell in water or biological fluids.⁴⁵ With n value of 0.5, the Korsmeyer-Peppas kinetics model for SL suggest that the drug release was primarily driven by fickian diffusion and $t^{0.51}$ dependent which is related to the conventional diffusion that organized by thermodynamic forces such as gradient of chemical potential and/or differences of concentrations with the constant diffusion coefficients, i.e. diffusion-controlled transport.

In vitro Hemolysis study

The phytosome are meant to be used either intravenously and/or orally. They interact with erythrocytes membrane upon intravenous injection, which may cause hemolysis of red blood cells. Therefore, *in vitro* hemolysis test is done prior to *in vivo* study. Hemolytic study was performed to indicate *in vitro* biocompatibility of phytosome to get an insight into the interaction of erythrocyte's membrane, which may trigger thrombosis, embolization or hemolysis. Bio-incompatible formulations can interact invisibly and cause lysis of the erythrocytes and release hemoglobin.⁴⁶ To verify the safety of SL and SPY, their hemolysis activities were investigated at high (1000 µg/ml), medium (100 µg/ml) and low (10 µg/ml) concentrations by incubation with normal RBC cells as an *in vitro* toxicity model. The results were given in Table 9. It was found that the hemolysis caused by SL is greater than 10% at higher concentration, whereas SPY is less than 10%. The present study showed that percent hemolysis for SPY was significantly less than SL at all concentration range. This is due to the encapsulation or entrapment of SL in phytosome. Generally, 10% of hemolysis caused by

Table 7: Stability studies of SPC and SPY.

Duration	Tem. (°C)	SPC						SPY			
		Complexation efficiency	% Reduction (Complexation efficiency)	Drug Loading	% Reduction (Drug Loading)	Drug content	% Reduction (Drug content)	Physical Appearance	Entrapment Efficiency	% Reduction (Entrapment Efficiency)	Physical Appearance
1 month	4	83.43 ± 0.40	0.42	70.26 ± 0.21	0.65	83.41 ± 0.13	1.17	Yellowish powder	93.15 ± 0.42	0.75	Yellowish suspension
	24	81.67 ± 0.89	2.52	66.08 ± 0.59	6.56	80.91 ± 0.15	4.13	Yellowish powder	90.71 ± 0.19	3.35	Yellowish suspension
2 month	4	83.54 ± 0.10	0.29	70.10 ± 0.03	0.87	83.91 ± 0.17	0.58	Yellowish powder	92.95 ± 0.42	0.96	Yellowish suspension
	24	79.78 ± 0.22	4.77	63.23 ± 0.29	10.59	79.26 ± 0.14	6.09	Yellowish powder	87.43 ± 0.41	6.85	Yellowish suspension
3 month	4	83.50±0.17	0.33	70.01±0.02	1.003	83.85±0.15	0.65	Yellowish powder	92.94±0.53	0.98	Yellowish suspension
	24	77.94 ± 0.65	6.97	61.66 ± 0.07	12.81	79.11 ± 0.59	6.26	Yellowish powder	84.68 ± 0.50	9.78	Yellowish suspension

Data were expressed as mean±SEM (n=3).

Table 8: The release kinetic models of SL and SPY respective to correlation coefficient.

Release kinetics models	Kinetic model parameter	Formulations	
		SIL	SPY
Zero order (F=k ₀ t)	k ₀	0.443	1.416
	Rsqr_adj	0.6606	0.9987
	AIC	42.8826	21.1756
	MSC	-0.1359	6.0072
First-order (F=100*[1-Exp(-k ₁ t)])	k ₁	0.005	0.024
	Rsqr_adj	0.7390	0.9315
	AIC	40.7826	52.6683
	MSC	0.1266	2.0706
Higuchi (F=kH*t ^{0.5})	kH	3.218	9.843
	Rsqr_adj	0.9799	0.8850
	AIC	20.2632	56.8116
	MSC	2.6916	1.5527
Korsmeyer-Peppas (F=kKP*t ⁿ)	kKP	4.773	1.623
	n	0.397	0.966
	Rsqr_adj	0.9931	0.9990
	AIC	12.4803	19.9176
Hixson-Crowell (F=100*[1-(1-kHC*t) ³])	kHC	0.002	0.007
	Rsqr_adj	0.7146	0.9630
	AIC	41.4971	47.7447
	MSC	0.0373	2.6861

Abbreviations: F, fraction of drug dissolved during the time t; k₀, zero-order release rate constant; k₁, first-order release rate constant; kH, Higuchi kinetic release rate constant; kKP, Korse Meyer-Peppas release rate constant; kHC; Hixson-Crowell release rate constant; n, release exponent.

Table 9: Percentage hemolysis of SL and SPY.

Concentration/drugs	Percentage hemolysis	
	SIL	SPY
10 µg/ml	6.788 ± 0.30	2.082 ± 0.34
100 µg/ml	9.848 ± 0.36	5.195 ± 0.30
1000 µg/ml	15.41 ± 0.33	7.133 ± 0.45

Data were expressed as mean±SEM (n=3).

any formulation is accepted as non-toxic and biocompatible.⁴⁷ Therefore, it can be concluded that SPY are non-toxic and biocompatible for *in vivo* administration.

In vitro membrane stabilizing activity

Harmful stimuli such as microorganism, toxic substances and tissue injury, initiates a tissue response called inflammation. Inflammation and oxidation are in close proximity: oxidation generates free radicals that damage cells leading to inflammation. Inflammation is a defensive mechanism that works in tandem with the healing process to counteract harmful stimuli. As a result, inflammation is a complicated physiologic state. Aging, cancer, adipogenesis, diabetes, cardiovascular difficulties, lung illness, and other diseases can all be caused by inflammation.⁴⁸ The anti-inflammatory term refers to the nature of chemical along with a treatment that can ameliorate inflammation. Membrane stabilization assay is a standard tool to study the antiinflammatory potential using erythrocytes.⁴⁹

In this study, the effect of SL, SPY and ASA were evaluated on hypotonic solution-induced hemolysis of RBC membrane for membrane stabilizing activity and found that SPY has significant membrane stabilization effect when compare to SL. Hypotonic solution cause swelling of erythrocytes, thus leads to hemolysis. SPY significantly inhibited hypotonic solution-induced hemolysis in a dose-dependent manner as shown in Table 10. The mode of action of membrane stabilization of SPY is due to

Table 10: Percentage inhibition of hemolysis by SIL and SPY.

Concentration	Hemolysis inhibition (%)		
	SL	SPY	ASA (200 µg/ml)
50µg/ml	48.23 ± 0.32	56.58 ± 0.42	70.49 ± 0.84
100 µg/ml	49.58 ± 0.27	66.60 ± 0.38	73.98 ± 0.76
200 µg/ml	51.11 ± 0.17	67.79 ± 1.48	77.58 ± 0.45
300 µg/ml	51.92 ± 0.25	77.78 ± 0.34	80.75 ± 0.77
500 µg/ml	53.16 ± 0.09	79.37 ± 0.83	84.49 ± 0.54

Data were expressed as mean±SEM (n=3).

an increase in the surface area/volume ratio by an enlargement of membrane or shrinkage of the cell, and an interaction with membrane proteins. Furthermore, the intracellular calcium level influences the deformability and cell volume of erythrocytes. As a result, it's possible that the phytosome's ability to modulate calcium influx is responsible for the protective effect on erythrocyte membrane.²⁷ The current study proposes that the membrane stabilizing activity of SPY has a significant role in its anti-inflammatory activity.

General Sign and Behavioral Analysis

An early assessment of toxic manifestations is one of the initial screening studies performed with all compounds during the examination of the toxic properties of any formulation or new chemical. Furthermore, the results of the acute toxicity research could be used to classify and label the test substance. As a result, it was believed that the current study would examine and focus on the acute and sub-acute toxicity of SPY in an animal model.

For both acute and sub-acute oral toxicity, oral treatment with SPY indicated no treatment-related death in both sexes. For all toxicity studies, physical examination of the SPY-treated rats revealed no symptoms of toxic consequences, such as changes in skin and fur, eyes and mucous membranes, behavior pattern, tremors, salivation, diarrhea, and coma. All animals in the acute and sub-acute oral toxicity groups showed no abnormalities.

Effect of SPY on body weight, relative organ weight, food consumption, water intake, and hematological and biochemical parameters in acute oral toxicity.

For any medicine intended for human use, acute toxicity studies in animals are required. The acute toxicity study has always been the first toxicity test undertaken. The fundamental goal of these investigations is to find a single dose that causes substantial side effects or life-threatening toxicity, which typically necessitates estimating the lethal dose. The experiments are normally conducted on rodents and consist of a single dose up to a maximum of 2000 mg/kg, or the maximum actually possible. In this study, SPY was found safe at a dose of 2000 mg/kg. This is the only study type in pharmaceutical drug development where lethality/life-threatening toxicity is a documented endpoint in current regulatory standards.⁵⁰

In this study, SPY was found safe at a dose of 2000 mg/kg. The steady increase in body weight was observed in both the control and SPY treated groups during the course of the study compared to the initial weight as given in Table 11. The percentage changes in body weight of the SPY treated groups were found significantly different compared to the control rats as $p < 0.05$. There was no statistically significant difference in relative organ weight between control and SPY treated groups of acute oral toxicity as shown in Table 12. The food consumption of all rats were normal. The food consumption between control and SPY treated groups were not found significant as $p > 0.05$ within two weeks (Table 13).

Table 11: Body weight and percentage change in body weight at 0 day, 1 and 2 week in acute oral toxicity.

Group	0 Day	Week 1	Week 2	% Change	
				Week 1	Week 2
Control	210.3 ± 2.90 ^{NS}	224.0 ± 2.08*	230.7 ± 3.180 ^{NS}	4.153 ± 1.62	9.683 ± 1.27
	SPY 50 mg/kg	225.0 ± 4.93 ^{NS}	237.3 ± 6.17 ^{NS}	246.3 ± 6.17 ^{NS}	2.187 ± 0.40
SPY 2000 mg/kg	224.7 ± 5.54 ^{NS}	235.0 ± 5.29 ^{NS}	243.0 ± 4.93 ^{NS}	1.853 ± 0.13	8.187 ± 0.75 **

Data were expressed as mean±SEM (n=3). The $P < 0.05$ was considered as significant (*), $p < 0.01$ considered as very significant (**), $p < 0.001$ considered as highly significant (***), and $p > 0.05$ considered as non-significant (^{NS}).

Table 12: The relative organ weight acute oral toxicity.

Groups	Control	SPY 50 mg/kg	SPY 2000 mg/kg
Brain	1.79 ± 0.06	1.78 ± 0.04 ^{NS}	1.78 ± 0.08 ^{NS}
Heart	0.4167 ± 0.014	0.3900 ± 0.005 ^{NS}	0.3867 ± 0.017 ^{NS}
Liver	2.873 ± 0.092	2.877 ± 0.071 ^{NS}	2.760 ± 0.078 ^{NS}
Kidney	0.7467 ± 0.012	0.7167 ± 0.012 ^{NS}	0.7333 ± 0.012 ^{NS}
Spleen	0.1933 ± 0.014	0.1900 ± 0.010 ^{NS}	0.1900 ± 0.005 ^{NS}
Lung	0.5367 ± 0.008	0.5233 ± 0.012 ^{NS}	0.5233 ± 0.012 ^{NS}

Data were expressed as mean±SEM (n=3). The $P < 0.05$ was considered as significant (*), $p < 0.01$ considered as very significant (**), $p < 0.001$ considered as highly significant (***), and $p > 0.05$ considered as non-significant (NS).

Table 13: Food consumption of the rats at 1 and 2 week acute oral toxicity.

Groups	Control	SPY	
		50 mg/kg	2000 mg/kg
Week 1	75.67 ± 1.309	74.21 ± 1.329 ^{NS}	82.22 ± 2.68 *
Week 2	77.08 ± 1.076	76.95 ± 1.003 ^{NS}	75.22 ± 1.298 ^{NS}

Data were expressed as mean±SEM (n=3). The $P < 0.05$ was considered as significant (*), $p < 0.01$ considered as very significant (**), $p < 0.001$ considered as highly significant (***), and $p > 0.05$ considered as non-significant (NS).

Table 14: Water intake of the rats at 1 and 2 week acute oral toxicity.

Groups	Control	SPY 50 mg/kg	SPY 2000 mg/kg
Week 1	112.6 ± 0.479	114.0 ± 0.673 ^{NS}	114.3 ± 0.800 ^{NS}
Week 2	112.5 ± 0.368	114.0 ± 0.667 ^{NS}	113.9 ± 0.757 ^{NS}

Data were expressed as mean±SEM (n=3). The $P < 0.05$ was considered as significant (*), $p < 0.01$ considered as very significant (**), $p < 0.001$ considered as highly significant (***), and $p > 0.05$ considered as non-significant (NS).

Similarly the water intake of control and SPY treated groups showed no statistically significant difference as $p > 0.05$ as shown in Table 14. The hematological profile and biochemical parameters of control and SPY treated groups summarized in Table 15. The results concluded that all hematological parameters such as CBC and differential blood count and biochemical parameter such as liver and renal function tests were within the normal range in both control and SPY treated groups. In ANOVA test, there is no significant association between the groups in acute toxicity tests as $p > 0.05$. According to the findings of this study, SPY has no acute toxicity effects and no rats have died as a result of it. Similarly,

Table 15: Hematological and Biochemical parameters of the rats in acute oral toxicity.

Parameter/Group	Control	SPY 50 mg/kg	SPY 2000 mg/kg
CBC			
HGB	144.7 ± 1.202	142.2 ± 3.087 ^{NS}	142.7 ± 2.028 ^{NS}
WBC	7.617 ± 0.093	7.690 ± 0.081 ^{NS}	7.653 ± 0.118 ^{NS}
Differential count			
Neutrophil	0.5200 ± 0.034	0.5767 ± 0.029 ^{NS}	0.5600 ± 0.011 ^{NS}
Lymphocyte	5.403 ± 0.083	5.860 ± 0.13 *	5.957 ± 0.13 *
Monocyte	0.1333 ± 0.008	0.1400 ± 0.005 ^{NS}	0.1600 ± 0.011 ^{NS}
Eosinophil	0.0800 ± 0.005	0.2767 ± 0.162 ^{NS}	0.09667 ± 0.008 ^{NS}
Basophil	0.0200 ± 0.005	0.02667 ± 0.008 ^{NS}	0.03333 ± 0.008 ^{NS}
Renal function test			
Urea	3.607 ± 0.173	3.883 ± 0.268 ^{NS}	3.700 ± 0.305 ^{NS}
Creatinine	31.67 ± 1.856	31.67 ± 1.453 ^{NS}	29.67 ± 0.881 ^{NS}
Liver function test			
Albumin	35.67 ± 1.453	38.00 ± 1.732 ^{NS}	35.67 ± 2.333 ^{NS}
Globulin	23.67 ± 0.666	23.00 ± 0.577 ^{NS}	23.00 ± 0.577 ^{NS}
Total bilirubin	1.067 ± 0.066	0.9667 ± 0.033 ^{NS}	1.033 ± 0.033 ^{NS}
Conjugate bilirubin	1	1	1
Alkaline phosphatase (ALP)	171.3 ± 0.666	168.3 ± 4.256 ^{NS}	172.0 ± 1.155 ^{NS}
Alanine Aminotransferase (ALT)	26.00 ± 1.528	25.67 ± 1.202 ^{NS}	26.67 ± 1.453 ^{NS}
Aspartate aminotransferase (AST)	96.00 ± 1.155	96.33 ± 4.372 ^{NS}	98.67 ± 5.207 ^{NS}

Data were expressed as mean±SEM (n=3). The $P < 0.05$ was considered as significant (*), $p < 0.01$ considered as very significant (**), $p < 0.001$ considered as highly significant (***), and $p > 0.05$ considered as non-significant (NS).

Table 16A: Body weight and percentage change in body weight in 4 weeks in sub-acute oral toxicity.

Group	0 week	Week 1	Week 2	Week 3	Week 4	Percentage change				
						Week 1	Week 2	Week 3	Week 4	
A Female rats										
Control	214.5 ± 2.09	233.7 ± 2.47 ***	248.3 ± 2.20 ***	260.7 ± 2.05 ***	268.0 ± 2.44 ***	8.960 ± 0.44	15.78 ± 0.49 ***	21.56 ± 1.00 ***	24.96 ± 1.27 ***	
SPY 500 mg/kg	205.9 ± 2.33	224.9 ± 3.20**	237.5 ± 3.59 ***	249.9 ± 3.15 ***	255.2 ± 4.01 ***	9.220 ± 0.37	15.34 ± 0.58 ***	21.36 ± 0.54 ***	23.92 ± 0.81 ***	
SPY 1000 mg/kg	208.9 ± 2.29	227.3 ± 3.56**	241.9 ± 2.87 ***	252.5 ± 2.49 ***	261.6 ± 1.56 ***	8.780 ± 0.55	15.78 ± 0.40 ***	20.88 ± 0.77 ***	25.24 ± 0.96 ***	
SPY 1500 mg/kg	212.3 ± 1.77	232.1 ± 2.80 ***	244.3 ± 3.42***	256.3 ± 3.68 ***	266.2 ± 5.91 ***	9.340 ± 0.61	15.04 ± 0.90 ***	20.68 ± 0.98 ***	25.36 ± 2.4 ***	
B Male rats										
Control	222.2 ± 2.74	234.6 ± 3.58 *	240.8 ± 4.55 ***	250.4 ± 3.75 ***	256.4 ± 4.34 ***	5.588 ± 1.21	8.372 ± 1.60 ^{NS}	12.71 ± 1.38 **	15.39 ± 1.37 ***	
SPY 500 mg/kg	208.4 ± 1.20	219.4 ± 1.8 ***	226.2 ± 2.78***	232.8 ± 3.89 ***	239.2 ± 3.41***	5.278 ± 0.54	8.536 ± 1.04*	11.69 ± 1.412**	14.76 ± 1.11 ***	
SPY 1000 mg/kg	203.6 ± 3.58	216.0 ± 3.74 *	220.2 ± 4.25 *	227.6 ± 3.01***	234.0 ± 2.89***	6.108 ± 0.86	8.172 ± 1.30 ^{NS}	11.85 ± 1.33**	15.01 ± 1.54**	
SPY 1500 mg/kg	207.2 ± 1.15	220.0 ± 3.34**	226.8 ± 3.08 ***	235.8 ± 4.25 ***	242.6 ± 4.02***	6.158 ± 1.10	9.450 ± 1.15 ^{NS}	13.78 ± 1.60**	15.87 ± 1.25***	

Data were expressed as mean±SEM (n=3). The $P < 0.05$ was considered as significant (*), $p < 0.01$ considered as very significant (**), $p < 0.001$ considered as highly significant (***), and $p > 0.05$ considered as non-significant (^{NS}).

a study conducted by Nashwan Abdullah *et al.* using *Dracaena cinnabari* resin methanol extract revealed that resin extract can be classified as category-5 in accordance with the Globally Harmonized System of Classification and Labelling of Chemicals, which has direct relevance for protecting human and animal health.³⁰

Effect of SPY on body weight, organ's weight, food consumption, water intake, and hematological and biochemical parameters in sub-acute oral toxicity.

Because cumulative toxic effects can occur even at very low dosages, acute toxicity data has limited clinical utility. As a result, multiple dose

studies are frequently used to assess the safety profile of drugs. As a result, the sub-acute test was employed. The LD₅₀ dose of acute toxicity was used to design this sub-acute toxicity study, and three different doses (500, 1000, and 1500 mg/kg) representing low, medium, and high doses, respectively, were tested in rats to see if there was no observable harmful effect.

In sub-acute toxicity study, the body weight of the control and SPY treated rats were as shown in Table 16. The body weight and percentage change in body weight of male and female rats gradually increase through the study period i.e. 4 week and 6week (Table 16A). The percentage changes

Table 16B: Body weight and percentage change in body weight in 6 weeks in sub-acute oral toxicity.

Group	0 week	Week 1	Week 2	Week 3	Week 4	Week 5	Week 6	Percentage change					
								Week 1	Week 2	Week 3	Week 4	Week 5	Week 6
A													
Female recovery groups													
Control	210.5 ± 2.28	218.7 ± 2.41 *	222.0 ± 2.16 **	226.6 ± 2.15***	233.0 ± 2.66 ***	241.0 ± 2.30***	246.6 ± 2.60 ***	3.920 ± 0.33	5.494 ± 0.30 **	7.684 ± 0.51 ***	10.72 ± 0.45 ***	14.53 ± 0.33 ***	17.18 ± 0.35 ***
SPY 1500 mg/kg	209.3 ± 2.98	218.3 ± 2.95 ^{NS}	220.2 ± 1.96 *	225.6 ± 2.20 **	231.2 ± 2.87 ***	238.6 ± 2.65 ***	243.6 ± 2.73 ***	4.338 ± 0.72	5.266 ± 0.61 ^{NS}	7.848 ± 0.74 **	10.51 ± 0.61 ***	14.06 ± 0.84 ***	16.44 ± 0.77 ***
B													
Female recovery groups													
Control	215.2 ± 1.6	226.4 ± 1.8 **	244.4 ± 2.61 ***	256.8 ± 1.93 ***	267.2 ± 1.71 ***	277.2 ± 2.05 ***	286.2 ± 3.26 ***	5.204 ± 0.34	13.57 ± 0.75 ***	19.34 ± 0.63 ***	24.18 ± 0.94 ***	28.83 ± 0.96 ***	33.00 ± 1.19***
SPY 1500 mg/kg	221.4 ± 1.72	232.4 ± 0.8 ***	251.0 ± 1.58 ***	267.0 ± 2.77 ***	277.6 ± 4.63 ***	287.6 ± 5.71 ***	295.8 ± 7.16***	4.984 ± 0.55	13.38 ± 0.35 ***	20.59 ± 0.61 ***	25.36 ± 1.41 ***	29.87 ± 1.84 ***	33.56 ± 2.51 ***

Data were expressed as mean±SEM (n=3). The $P < 0.05$ was considered as significant (*), $p < 0.01$ considered as very significant (**), $p < 0.001$ considered as highly significant (***), and $p > 0.05$ considered as non-significant (^{NS}).

Table 17A: The relative organ weight in sub-acute oral toxicity.

Organs/Groups	Control	SPY 500 mg/kg	SPY 1000 mg/kg	SPY 1500 mg/kg
A				
Female rats				
Brain	1.52 ± 0.012	1.56 ± 0.013 ^{NS}	1.54 ± 0.011 ^{NS}	1.52 ± 0.010 ^{NS}
Heart	0.41 ± 0.010	0.4200 ± 0.013 ^{NS}	0.41 ± 0.013 ^{NS}	0.4280 ± 0.012 ^{NS}
Liver	2.74 ± 0.0448	2.678 ± 0.0305 ^{NS}	2.65 ± 0.023 ^{NS}	2.734 ± 0.0297 ^{NS}
Kidney	0.75 ± 0.016	0.7740 ± 0.011 ^{NS}	0.78 ± 0.028 ^{NS}	0.7980 ± 0.019 ^{NS}
Spleen	0.22 ± 0.010	0.2280 ± 0.010 ^{NS}	0.23 ± 0.014 ^{NS}	0.2340 ± 0.012 ^{NS}
Lung	0.61 ± 0.009	0.6140 ± 0.011 ^{NS}	0.62 ± 0.006 ^{NS}	0.6380 ± 0.012 ^{NS}
B				
Male rats				
Brain	1.72 ± 0.08	1.76 ± 0.06 ^{NS}	1.74 ± 0.01 ^{NS}	1.72 ± 0.05 ^{NS}
Heart	0.44 ± 0.013	0.43 ± 0.011 ^{NS}	0.42 ± 0.014 ^{NS}	0.42 ± 0.016 ^{NS}
Liver	3.89 ± 0.0826	3.80 ± 0.073 ^{NS}	3.85 ± 0.112 ^{NS}	3.89 ± 0.066 ^{NS}
Kidney	0.97 ± 0.015	0.98 ± 0.012 ^{NS}	0.98 ± 0.012 ^{NS}	0.98 ± 0.013 ^{NS}
Spleen	0.23 ± 0.013	0.22 ± 0.014 ^{NS}	0.22 ± 0.016 ^{NS}	0.23 ± 0.011 ^{NS}
Lung	0.5295 ± 0.011	0.5308 ± 0.010 ^{NS}	0.5244 ± 0.0127 ^{NS}	0.5503 ± 0.006 ^{NS}

Data were expressed as mean±SEM (n=3). The $P < 0.05$ was considered as significant (*), $p < 0.01$ considered as very significant (**), $p < 0.001$ considered as highly significant (***), and $p > 0.05$ considered as non-significant (^{NS}).

in body weight of the SPY treated groups were not significant in first two weeks as $p > 0.05$, but in later weeks, it was found significant as $p < 0.05$. In addition, there is significant difference in body weight and percentage change in body weight of recovery groups in both male and female rats with $p < 0.05$ (Table 16B). There relative organ weight of control and SPY treated groups has no statistically significant difference in all group (Table 17A and B). The food consumption of all rats were normal. The food consumption in groups were not found significant as $p > 0.05$ (Table 18A, and B). Similarly the water intake of control and SPY treated rats in both female and male rats groups of sub-acute oral toxicity in 1st weeks showed significant difference as $p < 0.05$ whereas there is no significant difference in 2nd to 4th weeks female rats while male rats groups of sub-acute oral toxicity in 2nd weeks showed significant difference in

Table 17B: The relative organ weight in sub-acute oral toxicity.

Organs/Groups	Control	SPY 1500 mg/kg
A		
Female recovery groups		
Brain	1.73 ± 0.04	1.74 ± 0.09 ^{NS}
Heart	0.44 ± 0.010	0.44 ± 0.006 ^{NS}
Liver	2.96 ± 0.064	3.07 ± 0.079 ^{NS}
Kidney	0.84 ± 0.025	0.83 ± 0.023 ^{NS}
Spleen	0.23 ± 0.011	0.23 ± 0.009 ^{NS}
Lung	1.30 ± 0.033	1.28 ± 0.009 ^{NS}
B		
Male recovery groups		
Brain	1.76 ± 0.02	1.75 ± 0.07 ^{NS}
Heart	0.41 ± 0.010	0.44 ± 0.012 ^{NS}
Liver	3.48 ± 0.053	3.73 ± 0.147 ^{NS}
Kidney	0.96 ± 0.019	1.01 ± 0.036 ^{NS}
Spleen	0.24 ± 0.008	0.25 ± 0.009 ^{NS}
Lung	0.50 ± 0.008	0.52 ± 0.021 ^{NS}

Data were expressed as mean±SEM (n=3). The $P < 0.05$ was considered as significant (*), $p < 0.01$ considered as very significant (**), $p < 0.001$ considered as highly significant (***), and $p > 0.05$ considered as non-significant (^{NS}).

Table 18A: Food consumption of the rats in 4 weeks in sub-acute oral toxicity.

Groups	Control	SPY 500 mg/kg	SPY 1000 mg/kg	SPY 1500 mg/kg
A				
Female rats				
Week 1	83.44 ± 0.963	81.58 ± 1.874 ^{NS}	80.20 ± 2.271 ^{NS}	77.83 ± 2.543 ^{NS}
Week 2	83.02 ± 1.297	80.43 ± 1.053 ^{NS}	81.70 ± 0.947 ^{NS}	78.94 ± 1.739 ^{NS}
Week 3	86.59 ± 1.373	86.15 ± 1.174 ^{NS}	85.17 ± 1.417 ^{NS}	83.21 ± 1.390 ^{NS}
Week 4	88.69 ± 1.383	87.36 ± 1.224 ^{NS}	87.75 ± 1.254 ^{NS}	87.04 ± 1.047 ^{NS}
B				
Male rats				
Week 1	91.75 ± 0.457	91.46 ± 0.675 ^{NS}	91.43 ± 0.823 ^{NS}	89.59 ± 0.916 ^{NS}
Week 2	94.53 ± 0.426	93.97 ± 0.336 ^{NS}	93.86 ± 0.662 ^{NS}	92.62 ± 0.41 **
Week 3	93.92 ± 1.207	96.67 ± 1.295 ^{NS}	96.44 ± 0.904 ^{NS}	95.51 ± 1.103 ^{NS}
Week 4	91.85 ± 0.605	92.54 ± 1.250 ^{NS}	94.73 ± 1.747 ^{NS}	96.10 ± 1.73 *

Data were expressed as mean±SEM (n=3). The $P < 0.05$ was considered as significant (*), $p < 0.01$ considered as very significant (**), $p < 0.001$ considered as highly significant (***), and $p > 0.05$ considered as non-significant (^{NS}).

Table 18 B: Food consumption of the recovery groups rats in 6 weeks in sub-acute oral toxicity.

Groups	Control	SPY 1500 mg/kg
Female rats recovery groups		
Week 1	81.94 ± 2.268 ^{NS}	79.98 ± 1.904 ^{NS}
Week 2	83.69 ± 0.864 ^{NS}	82.77 ± 0.728 ^{NS}
Week 3	92.34 ± 1.407 ^{NS}	88.76 ± 1.734 ^{NS}
Week 4	93.71 ± 0.870 ^{NS}	92.47 ± 0.603 ^{NS}
Week 5	96.11 ± 0.900 ^{NS}	94.07 ± 1.174 ^{NS}
Week 6	95.43 ± 1.566 ^{NS}	93.24 ± 1.736 ^{NS}
Male rats recovery groups		
Week 1	91.95 ± 0.546	89.31 ± 1.442 ^{NS}
Week 2	94.79 ± 1.021	92.68 ± 0.589 ^{NS}
Week 3	94.18 ± 1.542	98.16 ± 0.706 [*]
Week 4	91.97 ± 0.249	92.54 ± 1.276 ^{NS}
Week 5	92.97 ± 0.614	91.89 ± 0.692 ^{NS}
Week 6	109.2 ± 3.107	107.5 ± 2.767 ^{NS}

Data were expressed as mean±SEM (n=3). The $P < 0.05$ was considered as significant (*), $p < 0.01$ considered as very significant (**), $p < 0.001$ considered as highly significant (***), and $p > 0.05$ considered as non-significant (^{NS}).

Table 19 A: Water intake of the rats in 4 weeks in sub-acute oral toxicity.

Groups	Control	SPY 500 mg/kg	SPY 1000 mg/kg	SPY 1500 mg/kg
Female rats				
Week 1	132.4 ± 0.158	135.5 ± 0.18 ^{***}	135.5 ± 0.14 ^{***}	135.5 ± 0.19 ^{***}
Week 2	133.3 ± 0.208	135.7 ± 0.170 ^{NS}	136.0 ± 0.154 ^{NS}	135.9 ± 0.154 ^{NS}
Week 3	134.4 ± 0.186	137.3 ± 0.248 ^{NS}	137.1 ± 0.229 ^{NS}	137.2 ± 0.289 ^{NS}
Week 4	135.0 ± 0.188	137.3 ± 0.324 ^{NS}	137.4 ± 0.237 ^{NS}	137.6 ± 0.229 ^{NS}
Male rats				
Week 1	133.2 ± 0.525	136.7 ± 0.77 ^{**}	136.6 ± 0.86 ^{**}	136.0 ± 0.74 ^{**}
Week 2	134.1 ± 0.442	137.3 ± 0.56 ^{***}	137.4 ± 0.55 ^{***}	136.5 ± 1.188
Week 3	135.2 ± 0.363	136.6 ± 1.117 ^{NS}	136.5 ± 1.151 ^{NS}	136.4 ± 1.144 ^{NS}
Week 4	135.9 ± 0.296	136.9 ± 1.111 ^{NS}	137.1 ± 1.224 ^{NS}	136.9 ± 1.011 ^{NS}

Data were expressed as mean±SEM (n=3). The $P < 0.05$ was considered as significant (*), $p < 0.01$ considered as very significant (**), $p < 0.001$ considered as highly significant (***), and $p > 0.05$ considered as non-significant (^{NS}).

500 mg and 1000 mg/kg group (Table 19A). The recovery groups of female rats showed significant difference in 2nd, 3rd, and 4th weeks as $p < 0.05$ (Table 19B/A) whereas no significant difference in 5th and 6th week. Similarly, the recovery groups of male rats showed significant difference in 1st, 2nd, 3rd, and 4th weeks as $p < 0.05$ (Table 19B/B) whereas no significant difference in 5th and 6th week. The hematological and biochemical considerations of all groups are summarized in Table 20A, B, C, and D. The results concluded that all hematological parameters and biochemical parameter were inside the normal range in all groups. In sub-acute toxicity testing, there is no significant relationship between all groups in the ANOVA test, with $p > 0.05$.

Changes in body weight are an indicator of negative effects, and losing more than 20% of an animal's body weight is considered essential and has been recognized as one of the ethical end-points in various international recommendations.⁵¹

Table 19 B: Water intake of the rats in 4 weeks in sub-acute oral toxicity.

Groups	Control	SPY 1500 mg/kg
A		
Female rat recovery group		
Week 1	138.4 ± 2.416	143.6 ± 0.7402 ^{NS}
Week 2	143.3 ± 0.698	145.0 ± 0.28 [*]
Week 3	143.8 ± 0.357	145.8 ± 0.37 ^{**}
Week 4	144.5 ± 0.415	145.9 ± 0.38 [*]
Week 5	145.7 ± 0.373	146.0 ± 0.258 ^{NS}
Week 6	146.5 ± 0.338	146.6 ± 0.256 ^{NS}
B		
Male rat recovery group		
Week 1	134.4 ± 0.154	135.9 ± 0.32 ^{**}
Week 2	134.9 ± 0.240	137.1 ± 0.41 ^{***}
Week 3	136.4 ± 0.329	138.3 ± 0.51 ^{**}
Week 4	137.5 ± 0.359	138.9 ± 0.45 [*]
Week 5	138.4 ± 0.417	139.0 ± 0.325 ^{NS}
Week 6	138.9 ± 0.482	139.3 ± 0.505 ^{NS}

Data were expressed as mean±SEM (n=3). The $P < 0.05$ was considered as significant (*), $p < 0.01$ considered as very significant (**), $p < 0.001$ considered as highly significant (***), and $p > 0.05$ considered as non-significant (^{NS}).

Histopathological observation

A histomorphological evaluation was carried out to detect structural changes in the tissues under observation. Microscopic examination of the vital organs including brain, heart, kidney, liver, lung and spleen of the rats in all the SPY treated and control groups for acute (Figure 8) and sub-acute oral toxicity group (Figure 9) did not find any gross clinical changes.

The histological analysis of brain did not find any sign of toxicity. The pinealocytes, glial cells and blood vessels were found in normal architecture in all the acute and sub-acute oral toxicity group. The histomorphology of the liver and kidney of the control and SPY treated groups and recovery groups, both male and female, showed with normal morphological architecture. Under microscopic examination, the liver of SPY treated animal exhibits normal cellular architecture without any distortions comparable to the control groups. Furthermore, signs of injury such as necrosis, congestion, fat accumulation, or hemorrhage near the central vein or sinusoids not detected. The hepatocytes arranged in cords and clearly visible. The histology of the liver displayed no blood cells lysis, or neutrophil infiltration in the acute and the sub-acute oral toxicity group. For the kidneys, histologically there was no morphological change for all SPY treated groups. The appearance of the glomerular construction showed normal similar to the control groups. The kidney seems to be usual in both rats. The glomeruli, distal, and proximal convoluted tubules appears usual in both rats. There was no no congestion or tubular atrophies in the kidney. In the acute and sub-acute oral toxicity groups, all nephron cells had clearly visible nucleoli. In both female and male rats of control and SPY treated, the heart displays normal cardiac fibers and lungs appear a normal alveolar arrangement with no inflammatory sign in acute and the sub-acute oral toxicity group. Likewise, the spleen display normal arrangement in all the rats of acute and sub-acute oral toxicity group. Overall, no abnormalities was seen in the brain, heart, kidney, liver, lungs, and spleen of the control and SPY treated groups of female and male rats with no treatment related alteration due to SPY.

Thus, the histomorphological assessment of the particular organs did not reveal any morphological aberrations that could be recognized to the oral administration of SPY to the rats.

Table 20 A: Hematological and biochemical parameters of the rats in sub-acute oral toxicity (Female).

Parameter/Group	Control	SPY 500 mg/kg	SPY 1000 mg/kg	SPY 1500 mg/kg
CBC				
HGB	157.4 ± 2.600	149.8 ± 3.105	149.4 ± 2.462	154.8 ± 2.634 ^{NS}
WBC	6.862 ± 0.252	7.340 ± 0.087	7.980 ± 0.26 *	7.940 ± 0.23 *
Differential count				
Neutrophil	0.6740 ± 0.048	0.7540 ± 0.036	0.8920 ± 0.036 **	0.9300 ± 0.074 *
Lymphocyte	8.142 ± 0.477	8.416 ± 0.557	8.710 ± 0.4442	9.290 ± 0.4864 ^{NS}
Monocyte	0.1800 ± 0.004	0.1740 ± 0.004	0.1820 ± 0.008000	0.1860 ± 0.009798 ^{NS}
Eosinophil	0.0840 ± 0.005	0.0880 ± 0.008	0.1020 ± 0.02223	0.1160 ± 0.016 ^{NS}
Basophil	0.0280 ± 0.002	0.0340 ± 0.005	0.0320 ± 0.005831	0.0300 ± 0.005 ^{NS}
Renal function test				
Urea	3.840 ± 0.304	4.040 ± 0.136	3.800 ± 0.2408	4.100 ± 0.339 ^{NS}
Creatinine	27.00 ± 1.643	29.20 ± 1.655	27.40 ± 1.327 ^{NS}	29.60 ± 1.631 ^{NS}
Liver function test				
Albumin	34.20 ± 1.158	34.00 ± 1.414	36.00 ± 1.414 ^{NS}	35.00 ± 1.483 ^{NS}
Globulin	23.40 ± 0.748	23.00 ± 0.836	24.60 ± 1.077 ^{NS}	24.60 ± 1.631 ^{NS}
Total bilirubin	1	1	1	1
Conjugate bilirubin	1	1	1	1
Alkaline phosphatase (ALP)	206.0 ± 6.269	207.0 ± 12.59	212.8 ± 9.805 ^{NS}	201.0 ± 6.458 ^{NS}
Alanine Aminotransferase (ALT)	23.80 ± 1.241	24.80 ± 1.068	26.60 ± 0.6782 ^{NS}	26.20 ± 1.068 ^{NS}
Aspartate aminotransferase (AST)	98.40 ± 3.341	101.6 ± 1.631	101.6 ± 0.9798 ^{NS}	102.6 ± 1.327 ^{NS}

Data were expressed as mean±SEM (n=3). The P<0.05 was considered as significant (*), p<0.01 considered as very significant (**), p<0.001 considered as highly significant (***), and p>0.05 considered as non-significant (NS).

Table 20 B: Hematological and biochemical parameters of the rats in sub-acute oral toxicity (Male).

Parameter/Group	Control	SPY 500 mg/kg	SPY 1000 mg/kg	SPY 1500 mg/kg
CBC				
HGB	153.2 ± 2.478	148.8 ± 2.478 ^{NS}	150.0 ± 5.148 ^{NS}	158.8 ± 5.774 ^{NS}
WBC	9.420 ± 0.462	9.500 ± 1.095 ^{NS}	9.660 ± 0.593 ^{NS}	9.560 ± 1.668 ^{NS}
Differential count				
Neutrophil	1.184 ± 0.051	1.212 ± 0.071 ^{NS}	1.230 ± 0.079 ^{NS}	1.342 ± 0.134 ^{NS}
Lymphocyte	9.860 ± 0.946	9.842 ± 0.745 ^{NS}	10.59 ± 0.888 ^{NS}	10.97 ± 0.931 ^{NS}
Monocyte	0.1820 ± 0.008	0.1720 ± 0.007 ^{NS}	0.1860 ± 0.018 ^{NS}	0.2060 ± 0.018 ^{NS}
Eosinophil	0.1020 ± 0.008	0.1060 ± 0.008 ^{NS}	0.1180 ± 0.008 ^{NS}	0.1220 ± 0.011 ^{NS}
Basophil	0.0820 ± 0.009	0.0600 ± 0.012 ^{NS}	0.0640 ± 0.011 ^{NS}	0.0640 ± 0.012 ^{NS}
Renal function test				
Urea	3.780 ± 0.261	3.940 ± 0.153 ^{NS}	4.160 ± 0.172 ^{NS}	4.200 ± 0.226 ^{NS}
Creatinine	26.20 ± 1.855	26.00 ± 1.140 ^{NS}	25.60 ± 3.092 ^{NS}	29.20 ± 1.855 ^{NS}
Liver function test				
Albumin	37.00 ± 1.000	36.60 ± 0.509 ^{NS}	38.20 ± 2.354 ^{NS}	36.60 ± 0.748 ^{NS}
Globulin	22.60 ± 0.509	23.00 ± 0.707 ^{NS}	23.20 ± 0.663 ^{NS}	23.20 ± 0.583 ^{NS}
Total bilirubin	1	1	1	1
Conjugate bilirubin	1	1	1	1
Alkaline phosphatase (ALP)	218.2 ± 7.599	220.4 ± 5.680 ^{NS}	224.4 ± 8.280 ^{NS}	238.4 ± 5.697 ^{NS}
Alanine aminotransferase (ALT)	31.60 ± 1.470	31.40 ± 0.678 ^{NS}	31.60 ± 1.030 ^{NS}	34.00 ± 1.265 ^{NS}
Aspartate aminotransferase (AST)	106.8 ± 2.990	108.0 ± 1.761 ^{NS}	107.4 ± 2.482 ^{NS}	111.0 ± 2.214 ^{NS}

Data were expressed as mean±SEM (n=3). The P<0.05 was considered as significant (*), p<0.01 considered as very significant (**), p<0.001 considered as highly significant (***), and p>0.05 considered as non-significant (NS).

Table 20 C: Hematological and biochemical parameters of the rats in recovery groups for sub-acute oral toxicity (Female)

Parameter/Group	Control	SPY 1500 mg/kg
CBC		
HGB	158.0 ± 3.050	157.8 ± 2.672 ^{NS}
WBC	7.000 ± 0.320	7.040 ± 0.269 ^{NS}
Differential count		
Neutrophil	1.284 ± 0.050	1.362 ± 0.047 ^{NS}
Lymphocyte	9.326 ± 0.425	9.342 ± 0.315 ^{NS}
Monocyte	0.2480 ± 0.022	0.2560 ± 0.014 ^{NS}
Eosinophil	0.1240 ± 0.008	0.1320 ± 0.011 ^{NS}
Basophil	0.0540 ± 0.005	0.0580 ± 0.003 ^{NS}
Renal function test		
Urea	3.990 ± 0.314	4.090 ± 0.0748 ^{NS}
Creatinine	31.40 ± 1.364	29.20 ± 1.772 ^{NS}
Liver function test		
Albumin	36.20 ± 1.241	34.40 ± 1.503 ^{NS}
Globulin	24.00 ± 0.707	23.20 ± 0.583 ^{NS}
Total bilirubin	2	2 ^{NS}
Conjugate bilirubin	1	1 ^{NS}
Alkaline phosphatase (ALP)	186.4 ± 13.02	192.4 ± 13.06 ^{NS}
Alanine aminotransferase (ALT)	27.20 ± 0.800	27.60 ± 0.927 ^{NS}
Aspartate aminotransferase (AST)	105.4 ± 1.470	107.0 ± 1.225 ^{NS}

Data were expressed as mean±SEM (n=3). The $P < 0.05$ was considered as significant (*), $p < 0.01$ considered as very significant (**), $p < 0.001$ considered as highly significant (***), and $p > 0.05$ considered as non-significant (^{NS}).

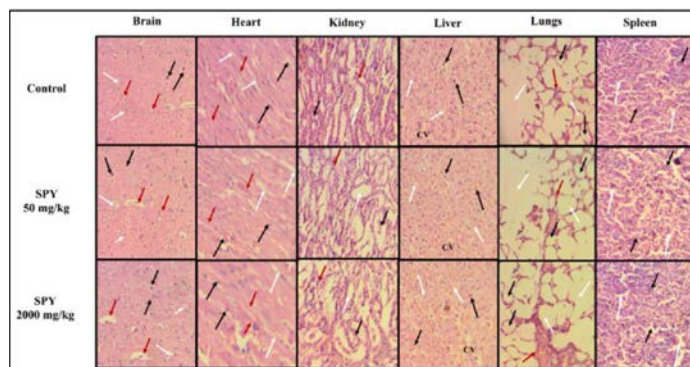


Figure 8: Photomicrograph of vital organs in acute oral toxicity (H&E Stain, ×40). Brain: black arrow – pinealocytes; white arrow – glial cells; red arrow – blood vessels. Heart: black arrow – central nucleus; white arrow – connective tissue; red arrow – muscle fiber. Kidney: black arrow – glomerulus; white arrow – macula densa; red arrow – blood vessels. Liver: black arrow – Hepatocytes; white arrow – sinusoidal space; CV- central vein. Lung: Black arrow – bronchiole; white arrow – alveolar sac; red arrow – Capillaries. Spleen: Black arrow – red pulp, white arrow – white pulp.

CONCLUSION

According to the findings of this investigation, PLs-base molecular complexes have a promising potential for increasing solubility and dissolution. A comprehensive factorial design technique was used to direct the phytosome preparation, combining particular factor and

Table 20 D: Hematological and biochemical parameters of the rats in recovery groups for sub-acute oral toxicity (male).

Parameter/Group	Control	SPY 1500 mg/kg
CBC		
HGB	150.4 ± 3.043	151.2 ± 3.338 ^{NS}
WBC	9.100 ± 0.606	10.56 ± 0.549 ^{NS}
Diff count		
Neutrophil	0.8780 ± 0.056	1.112 ± 0.104 ^{NS}
Lymphocyte	9.973 ± 0.334	9.148 ± 2.101 ^{NS}
Monocyte	0.1920 ± 0.027	0.2033 ± 0.027 ^{NS}
Eosinophil	1.785 ± 1.573	2.092 ± 1.880 ^{NS}
Basophil	0.0780 ± 0.006	0.09333 ± 0.014 ^{NS}
Renal function test		
Urea	3.760 ± 0.153	3.277 ± 0.647 ^{NS}
Creatinine	23.00 ± 1.732	20.36 ± 4.269 ^{NS}
Liver function test		
Albumin	33.20 ± 0.583	27.03 ± 5.408 ^{NS}
Globulin	18.20 ± 0.374	14.53 ± 2.915 ^{NS}
Total bilirubin	1	1 ^{NS}
Conjugate bilirubin	1	1 ^{NS}
Alkaline phosphatase (ALP)	221.6 ± 13.41	224.2 ± 12.68 ^{NS}
Alanine Aminotransferase (ALT)	29.00 ± 1.517	28.00 ± 1.703 ^{NS}
Aspartate aminotransferase (AST)	105.0 ± 2.702	109.4 ± 2.657 ^{NS}

Data were expressed as mean±SEM (n=3). The $P < 0.05$ was considered as significant (*), $p < 0.01$ considered as very significant (**), $p < 0.001$ considered as highly significant (***), and $p > 0.05$ considered as non-significant (^{NS}).

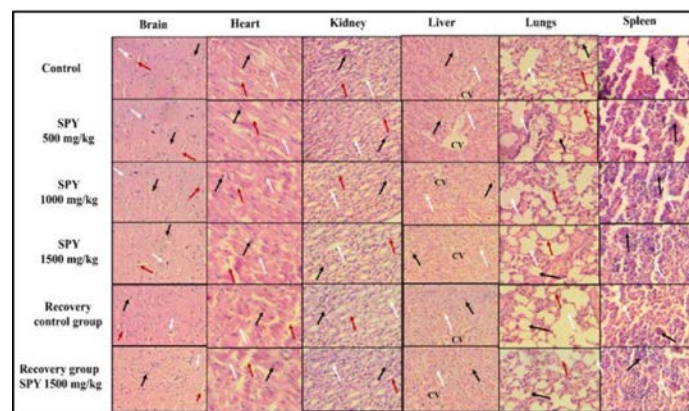


Figure 9: Photomicrograph of vital organs in sub-acute oral toxicity H&E Stain, ×40). Brain: black arrow – pinealocytes; white arrow – glial cells; red arrow – blood vessels. Heart: black arrow – central nucleus; white arrow – connective tissue; red arrow – muscle fiber. Kidney: black arrow – glomerulus; white arrow – macula densa; red arrow – blood vessels. Liver: black arrow – Hepatocytes; white arrow – sinusoidal space; CV- central vein. Lung: Black arrow – bronchiole; white arrow – alveolar sac; red arrow – Capillaries. Spleen: Black arrow – red pulp, white arrow – white pulp.

process variables to give an optimum result. The presence of non-covalent bonding interactions, such as hydrogen bonding, ion-dipole, and van der Waals interactions are key factors in the formation of a stable SPY, which were confirmed by FTIR, DSC, PXRD, and 1H NMR. When compared to pure SL, the optimized formulation was found to

have better water solubility of SPY. In dissolution experiments, the formulation also demonstrated a much higher rate and extent of SL release. At all concentrations, the percentage hemolysis for SPY was substantially lower than SL. As a result, it may be inferred that SPY are non-toxic and biocompatible for *in vivo* administration. SPY significantly inhibited hypotonic solution-induced hemolysis in a dose-dependent manner. In acute oral toxicity, no treatment-related death or toxic signs were observed. The SPY could be classed as Category 5 since it was well tolerated up to a dose of 2000 mg/kg body weight. Up to a higher dose level, the sub-acute test observations indicate no treatment-related abnormalities. There were no anomalies in food consumption, body weight, organ weight, hematological parameters, biochemical parameters, or histological investigation. The study reveals that using PL-based phytosomes to improve SL distribution is a feasible and realistic method.

Funding

This research was financially supported by Human Resource Development Group (HRDG) Council of Scientific and Industrial Research, New Delhi grant number: 09/150(0136)/19-EMR-I.

ACKNOWLEDGEMENT

We thank Dr. Aasheesh Srivastava, Associate Professor, Dept. of Chemistry, IISER Bhopal for providing the DLS and TEM facility to carry out the research work. Authors are also thankful to the Sophisticated Instrumentation Center (SIC), Dr. Harisingh Gour Vishwavidyalaya, Sagar for sophisticated instrumentation facilities supported under DST-PURSE (II).

Authors Contribution

Mandeep Kumar Singh conceived of the study, developed it, carried out the experiments, analyzed the results, and wrote the first draught of the publication. The article was monitored, corrected, and edited by Umesh Kumar Patil. The final text was reviewed and approved by both authors.

CONFLICT OF INTEREST

The authors declare that there is no conflict of interest.

REFERENCES

- Pourová J, Applová L, Macáková K, Vopršalová M, Migkos T, Bentanachs R, *et al.* The effect of silymarin flavonolignans and their sulfated conjugates on platelet aggregation and blood vessels *ex vivo*. *Nutrients*. 2019;11(10). doi: 10.3390/nu11102286, PMID 31554252.
- Bijak M. Silybin, a Major Bioactive Component of Milk Thistle (*Silybum marianum* L. Gaertn.)-Chemistry, Bioavailability, and Metabolism. *Molecules*. 2017;22(11):1-11. doi: 10.3390/molecules22111942, PMID 29125572.
- Song IS, Nam SJ, Jeon JH, Park SJ, Choi MK. Enhanced bioavailability and efficacy of silymarin solid dispersion in rats with acetaminophen-induced hepatotoxicity. *Pharmaceutics*. 2021;13(5). doi: 10.3390/pharmaceutics13050628, PMID 33925040.
- Sornsuvit C, Hongwiset D, Yotsawimonwat S, Toonkum M, Thongsawat S, Taesotikul W. The bioavailability and pharmacokinetics of silymarin SMEDDS formulation study in healthy Thai volunteers. *Evid Based Complement Alternat Med*. 2018;2018:1507834. doi: 10.1155/2018/1507834, PMID 30108644.
- Di Costanzo A, Angelico R. Drug delivery strategies for poorly water-soluble silymarin *Prime Arch*. *Mol Biol*. 2020;1-60. doi: 10.37247/pamb.1.2020.28.
- Lu M, Qiu Q, Luo X, Liu X, Sun J, Wang C, *et al.* Phyto-phospholipid complexes (phytosomes): A novel strategy to improve the bioavailability of active constituents. *Asian J Pharm Sci*. 2019;14(3):265-74. Doi: 10.1016/j.ajps.2018.05.011, PMID 32104457.
- Hou Z, Li Y, Huang Y, Zhou C, Lin J, Wang Y, *et al.* Phytosomes loaded with Mitomycin C-soybean phosphatidylcholine complex developed for drug delivery. *Mol Pharm*. 2013;10(1):90-101. doi: 10.1021/mp300489p, PMID 23194396.
- Amit G, Ashawat MS, Shailendra S, Swarnlata S. Phytosome: A novel approach towards functional cosmetics. *J Plant Sci*. 2007;2(6):644-9. doi: 10.3923/jps.2007.644.649.
- Wen H, Jung H, Li X. Drug delivery approaches in addressing Clinical Pharmacology-related issues: Opportunities and challenges. *AAPS J*. 2015;17(6):1327-40. doi: 10.1208/s12248-015-9814-9, PMID 26276218.
- Priya LB, Baskaran R, Padma VV, Chapter 21. Phytanoconjugates in oral medicine. In: *Nanostructures oralmed Elsevier inc*; 2017. p. 639-68. doi: 10.1016/B978-0-323-47720-8/00022-5.
- Kidd P, Head K. A review of the bioavailability and clinical efficacy of milk thistle phytosome: A silybin-phosphatidylcholine complex (Siliiphos). *Altern Med Rev*. 2005;10(3):193-203. PMID 16164374.
- Bhardwaj S, Gupta D. Study of acute, Sub acute and chronic toxicity test. *Int J Curr Biomed Pharm Res*. 2012;2:103-29.
- Sahu SC, Hayes AW. Toxicity of nanomaterials found in human environment. *Toxicol Res Appl*. 2017;1. doi: 10.1177/2397847317726352.
- U.S.D. of H. and H. Services, Guidance for industry and review staff – non-clinical safety evaluation of reformulated drug products and products intended for administration by an alternate route, 2008.
- M. of S. and T. Department of Biotechnology, Guidelines for evaluation of Nanopharmaceuticals in India; 2019. Available from: http://dbtindia.gov.in/sites/default/files/uploadfiles/Guidelines_For_Evaluation_of_Nanopharmaceuticals_in_India_24.10.19.pdf [cited 30/6/2022]. In:.
- Saoji SD, Raut NA, Dhore PV, Borkar CD, Popielarczyk M, Dave VS. Preparation and evaluation of phospholipid-based complex of standardized Centella extract (SCE) for the enhanced delivery of phytoconstituents. *AAPS J*. 2016;18(1):102-14. doi: 10.1208/s12248-015-9837-2, PMID 26563253.
- Chi C, Zhang C, Liu Y, Nie H, Zhou J, Ding Y. Phytosome-nanosuspensions for silybin-phospholipid complex with increased bioavailability and hepatoprotection efficacy. *Eur J Pharm Sci*. 2020;144:105212. doi: 10.1016/j.ejps.2020.105212, PMID 31923602.
- Bhattacharyya S, Reddy P. Effect of surfactant on azithromycin dihydrate loaded stearic acid solid lipid nanoparticles. *Turk J Pharm Sci*. 2019;16(4):425-31. doi: 10.4274/tjps.galenos.2018.82160, PMID 32454745.
- Haider T, Dubey S, Kanwar InduL. Preparation, optimization and *in vitro* studies of spectrin decorated liposomes: A promising strategy for cancer treatment. *Trends Pept Protein Sci*. 2021;V(P). and V.S:88-98. doi: 10.22037/tpps.v6i.36423.
- Anwar E, Farhana N. Formulation and evaluation of Phytosome-loaded maltodextrin-gum arabic microsphere system for delivery of Camellia sinensis extract. *J Young Pharm*. 2018;10(2s):S56-62. doi: 10.5530/jyp.2018.2s.11.
- Yanyu X, Yunmei S, Zhipeng C, Qineng P. The preparation of silybin-phospholipid complex and the study on its pharmacokinetics in rats. *Int J Pharm*. 2006;307(1):77-82. doi: 10.1016/j.ijpharm.2005.10.001, PMID 16300915.
- Zeng QP, Liu ZH, Huang A-W, Zhang J, Song HT. Preparation and characterization of silymarin synchronized-release microporous osmotic pump tablets. *Drug Des Devel Ther*. 2016;10:519-31. doi: 10.2147/DDDT.S91571, PMID 26889080.
- Sahoo RK, Biswas N, Guha A, Sahoo N, Kuotsu K. Development and *in vitro/in vivo* evaluation of controlled release vesicles of a nateglinide–maltodextrin complex. *Acta Pharm Sin B*. 2014;4(5):408-16. doi: 10.1016/j.apsb.2014.08.001, PMID 26579411.
- Haider T, Pandey V, Behera C, Kumar P, Gupta PN, Soni V. Spectrin conjugated PLGA nanoparticles for potential membrane phospholipid interactions: Development, optimization and *in vitro* studies. *J Drug Deliv Sci Technol*. 2020;60:102087. doi: 10.1016/j.jddst.2020.102087.
- Yang G, Zhao Y, Zhang Y, Dang B, Liu Y, Feng N. Enhanced oral bioavailability of silymarin using liposomes containing a bile salt: Preparation by supercritical fluid technology and evaluation *in vitro* and *in vivo*. *Int J Nanomedicine*. 2015;10:6633-44. doi: 10.2147/IJN.S92665, PMID 26543366.
- Nuruki Y, Matsumoto H, Tsukada M, Tsukahara H, Takajo T, Tsuchida K, *et al.* Method to improve azo-compound (AAPH)-Induced Hemolysis of Erythrocytes for Assessing Antioxidant Activity of lipophilic compounds. *Chem Pharm Bull (Tokyo)*. 2021;69(1):67-71. doi: 10.1248/cpb.c20-00568, PMID 33390522.
- Shinde UA, Phadke AS, Nair AM, Mungantiwar AA, Dikshit VJ, Saraf MN. Membrane stabilizing activity - A possible mechanism of action for the anti-inflammatory activity of Cedrus deodara wood oil. *Fitoterapia*. 1999;70(3):251-7. doi: 10.1016/S0367-326X(99)00030-1.
- OECD, OECD. Guideline for testing of chemicals. Acute oral toxicity-acute toxic class method, guideline no. 423; n.d.
- Repeated Dose 28-Day Oral Toxicity Study in Rodents (OECD TG 407). *OECD Series on Testing and Assessment*. 2018:477-90. doi: 10.1787/9789264304741-22-en.
- Al-Affifi NA, Alabsi AM, Bakri MM, Ramanathan A. Acute and sub-acute oral toxicity of *Dracaena cinnabari* resin methanol extract in rats. *BMC Complement Altern Med*. 2018;18(1):50. doi: 10.1186/s12906-018-2110-3, PMID 29402248.
- Jain P, Taleuzzaman M, Kala C, Kumar Gupta DK, Ali A, Aslam M. Quality by design (Qbd) assisted development of phytosomal gel of aloe vera extract for topical delivery. *J Liposome Res*. 2021;31(4):381-8. doi: 10.1080/08982104.2020.1849279, PMID 33183121.
- Maryana W, Rachmawati H, Mudhakir D. Formation of phytosome containing silymarin using thin layer-hydration technique aimed for oral delivery. *Mater Today Proc*. 2016;3(3):855-66. doi: 10.1016/j.matpr.2016.02.019.
- Liang J, Liu Y, Liu J, Li Z, Fan Q, Jiang Z, *et al.* Chitosan-functionalized lipid-polymer hybrid nanoparticles for oral delivery of silymarin and enhanced lipid-lowering effect in NAFLD. *J Nanobiotechnology*. 2018;16(1):64. doi: 10.1186/

- s12951-018-0391-9, PMID 30176941.
34. Y. ze LIU, D.Y. wei LEE, Standardization and Identification of Minor Components of silymarin (MK-001). *Chin Herb Med.* 2012;4:237-44. doi: 10.3969/j.issn.1674-6384.2012.03.011.
 35. Danaei M, Dehghankhold M, Ataei S, Hasanzadeh Davarani F, Javanmard R, Dokhani A, *et al.* Impact of particle size and polydispersity index on the clinical applications of lipidic nanocarrier systems. *Pharmaceutics.* 2018;10(2):1-17. doi: 10.3390/pharmaceutics10020057, PMID 29783687.
 36. Glassman PM, Muzykantov VR. Pharmacokinetic and pharmacodynamic properties of drug delivery systems. *J Pharmacol Exp Ther.* 2019;370(3):570-80. doi: 10.1124/jpet.119.257113, PMID 30837281.
 37. Gaikwad VL, Choudhari PB, Bhatia NM, Bhatia MS. Characterization of pharmaceutical nanocarriers: *In vitro* and *in vivo* studies. In: *Nanomater drug deliv ther.* Elsevier Inc; 2019. p. 33-58. doi: 10.1016/B978-0-12-816505-8.00016-3.
 38. Ong SGM, Ming LC, Lee KS, Yuen KH. Influence of the encapsulation efficiency and size of liposome on the oral bioavailability of griseofulvin-loaded liposomes. *Pharmaceutics.* 2016;8(3). doi: 10.3390/pharmaceutics8030025, PMID 27571096.
 39. Saputra YE, Dzakwan M, Dewi NA. Evaluation Nano-phytosome of myricetin with thin layer film hydration-sonication method. In: *Proceedings of the 2nd Bakti Tunas Husada-Health Sci international conference (BTH-HSIC 2019).* Paris, France: Atlantis Press; 2020. p. 294-7. doi: 10.2991/ahsr.k.200523.070.
 40. Mittal B. Pharmacokinetics and preformulation, how to dev. Robust solid oral dos. *Forms Concept Post-Approval.* 2017;17-37. doi: 10.1016/B978-0-12-804731-6.00002-9.
 41. Cumming H, Rücker C. Octanol-water partition coefficient measurement by a simple ¹H NMR method. *ACS Omega.* 2017;2(9):6244-9. doi: 10.1021/acsomega.7b01102, PMID 31457869.
 42. Papich MG, Martinez MN. Applying Biopharmaceutical Classification System (BCS) criteria to predict oral absorption of drugs in dogs: Challenges and pitfalls. *AAPS J.* 2015;17(4):948-64. doi: 10.1208/s12248-015-9743-7, PMID 25916691.
 43. Zhang Y, Huo M, Zhou J, Zou A, Li W, Yao C, *et al.* DDSolver: An add-in program for modeling and comparison of drug dissolution profiles. *AAPS J.* 2010;12(3):263-71. doi: 10.1208/s12248-010-9185-1, PMID 20373062.
 44. Dash S, Murthy PN, Nath L, Chowdhury P. Kinetic modeling on drug release from controlled drug delivery systems. *Acta Pol Pharm.* 2010;67(3):217-23. PMID 20524422.
 45. Solanki D, Motiwale M, Mahapatra S. Study of drug release kinetics from sustained release matrix tablets of acyclovir using natural polymer obtained from *Colocasia esculenta*. *Int J Pharm Tech Res.* 2020;13(3):172-9. Doi: 10.20902/IJPTR.2019.130306.
 46. Lakkadwala S, Singh J. Co-delivery of doxorubicin and erlotinib through liposomal nanoparticles for glioblastoma tumor regression using an *in vitro* brain tumor model. *Colloids Surf B Biointerfaces.* 2019;173:27-35. Doi: 10.1016/j.colsurfb.2018.09.047, PMID 30261346.
 47. Elmowafy M, Viitala T, Ibrahim HM, Abu-Elyazid SK, Samy A, Kassem A, *et al.* Silymarin loaded liposomes for hepatic targeting: *In vitro* evaluation and HepG2 drug uptake. *Eur J Pharm Sci.* 2013;50(2):161-71. doi: 10.1016/j.ejps.2013.06.012, PMID 23851081.
 48. Chaity FR, Khatun M, Rahman MS. *In vitro* membrane stabilizing, thrombolytic and antioxidant potentials of *Drynaria quercifolia* L., a remedial plant of the Garo tribal people of Bangladesh. *BMC Complement Altern Med.* 2016;16:184. doi: 10.1186/s12906-016-1170-5, PMID 27378075.
 49. Yesmin S, Paul A, Naz T, Rahman ABMA, Akhter SF, Wahed Mill, *et al.* Membrane stabilization as a mechanism of the anti-inflammatory activity of ethanolic root extract of Choi (Piper chaba). *Clin Phytosci.* 2020;6(1). Doi: 10.1186/s40816-020-00207-7.
 50. Robinson S, Delongea JL, Donald E, Dreher D, Festag M, Kervyn S, *et al.* A European pharmaceutical company initiative challenging the regulatory requirement for acute toxicity studies in pharmaceutical drug development. *Regul Toxicol Pharmacol.* 2008;50(3):345-52. doi: 10.1016/j.yrtph.2007.11.009. PMID 18295384.
 51. OECD. OECD guidance document on the recognition, assessment, and use of clinical signs as humane endpoints for experimental animals used in safety evaluation; 2000.

Article History: Submission Date : 06-05-2022; Revised Date : 09-06-2022; Acceptance Date : 25-06-2022.

Cite this article: Singh MK, Patil UK. Development and Characterization of Silymarin Phospholipid Complex for Improved Solubility, and Toxicological Evaluation in Experimental Animals. *Int. J. Pharm. Investigation.* 2022;12(3):299-316.